Flexible Towpreg for the Fabrication of High Thermal Conductivity Carbon/Carbon Composites

James W. Klett and Dan D. Edie
Department of Chemical Engineering and Center for Advanced Engineering Fibers
Clemson University, Clemson, SC, USA, 29634-0909

Abstract - A continuous powder coating process was used to produce flexible, pre-impregnated towpreg from a heat treated Mitsubishi AR mesophase pitch powder (AR-120) and three different carbon fibers: T300 PAN-based fiber, P55 pitch-based fiber, and an experimental high thermal conductivity pitch-based ribbon fiber. The towpreg then was hot-pressed into unidirectional composites, oxidized, carbonized at 1100°C, and then graphitized at 2400°C.

As expected, the PAN-based fibers developed strong fiber/matrix bonding and the pitch-based fibers developed poor fiber/matrix bonding. This resulted in high flexural strengths (841 MPa) in the graphitized composites reinforced with the T300 fibers and low flexural strengths (196 MPa) in the graphitized composites reinforced with the P55 fibers. In addition, it was found that during consolidation the ribbon fibers oriented normal to the pressing direction.

The thermal conductivity (parallel to the fibers) of the graphitized T300/AR-120 and P55/AR-120 composites was 80.5 and 135.5 W/m·K, respectively. These results, along with x-ray analysis, indicated a significant development of preferred crystalline order (parallel to the fibers) upon graphitization at 2400°C. The composites reinforced with ribbon fibers exhibited 3-D anisotropy, with a thermal conductivity (transverse to the fibers) of 213.5 W/m·K, higher than that parallel to the fibers (145 W/m·K). These results indicated that fiber shape can affect matrix properties in carbon/carbon composites.

Finally, the towpreg was woven into a 2-D fabric, demonstrating that towpreg can be used to produce preimpregnated multidimensional composite preforms. Towpreg may provide a low-cost route for producing carbon/carbon composites materials.

Key Words - carbon/carbon, powder coating, towpreg, mesophase, oxidation

1. INTRODUCTION

Currently, most carbon/carbon composites are made from carbon fiber-reinforced phenolic-based resins and require numerous costly densification cycles. However, many researchers have evaluated the use of high carbon content pitch resins as the matrix material. The objective is to reduce the number of densification cycles and, thus, the composite's cost. Unfortunately, the high viscosity of these pitches prevents them from completely penetrating the fine pores in the fiber bundles which make up the composites. The result is a composite which is often less dense, contains more voids, and has lower mechanical properties than those formed from phenolic-based resins. Poor infiltration, caused by high resin viscosity, also is a problem for the new generation of high temperature thermoplastic resins used to manufacture polymeric composites. To overcome the infiltration problem, Gantt and Allen developed a powder coating process for applying high-viscosity thermoplastic resins to carbon fiber tows [1, 2].

In their process the carbon fiber was unwound from a supply spool and passed over a tension-control device. Then, the fiber bundle was separated using a vacuum spreader and passed through a fluidization chamber where fine polymer particles were deposited onto the individual filaments of the spread tow. Next, the coated tow entered a tube furnace where the polymer particles were fused to the individual filaments of the tow. This process produced a coated fiber towpreg which was more flexible than prepreg produced by conventional melt, slurry, or solvent coating processes. In fact, this towpreg was flexible enough to be woven, braided, and knitted into multidimensional textile preforms. Since the textile preform was fabricated with pre-coated carbon fibers, it could be hot-pressed directly to form the final composite, eliminating the need for melt impregnation.

The objective of the current research was to explore possible low-cost routes for producing high thermal conductivity carbon/carbon composites. The powder coating process appeared to be well-suited for producing a preimpregnated carbon/carbon tow. Therefore, at the beginning of the project the critical parameters for towpreg production and subsequent composite fabrication were identified and optimized. These included the composition of the matrix pitch and the procedures used to press, oxidize and carbonize the composites. Three different types of carbon fibers were formed into towpreg, demonstrating that the process can be used to coat a variety of carbon fibers. Then, composites were made from the three different types of towpreg, and the final mechanical and thermal properties of the composites evaluated.

2. MATERIALS

Three types of fibers were selected for this research: T300 PAN-based carbon fiber [3], P55 pitch-based fiber [3], and an experimental high thermal conductivity ribbon-shaped fiber produced from Mitsubishi AR mesophase [4]. These three types of fibers were utilized, not only because they demonstrated the versatility of the coating process, but also because they are known to exhibit different degrees of interfacial bonding. Therefore, the composite results should provide data on the effect of interface structure on thermal conductivity. The properties of the as-received fibers are listed in Table 1. However, because the composites made with these fibers will be heat treated to 2400°C, one might expect the mechanical and thermal properties of these fibers will change during the firing process. Therefore, separate groups of the fibers were heat treated to

2400°C. After heat-treatment, the mechanical and thermal properties were measured by single filament testing, and these results are also presented in Table 1.

Table 1. Treatment conditions and final properties of fibers used in carbon/carbon composites.

	T300		P55		Type I Ribbon	Type II Ribbon
Heat Treatment Temperature (°C)	as-received	2400	as-received	2400	2400	2400
Cross Sectional Area (μm^2)	42	38	78	65	335	335
Density (g/cc)	1.76	1.81	2.0	2.0	2.2	2.2
Electrical Resistivity[a] ($\mu\Omega m$)	18	9.3	8.6	6.4	5.7	3.5
Thermal Conductivity[b] (W/mK)	8.5	76	98	196	236	429
Tensile Strength[c] (GPa)	3.0	1.8	1.8	2.1	2.1	2.6
Elongation at Break[c] (%)	1.3	0.6	0.5	--	--	--
Tensile Modulus[c] (GPa)	221	302	403	500	--	--
Sizing	no	no	no	no	no	no
Surface Treatment	yes	yes	yes	yes	no	no

[a] Single filament resistivity test (average value for 24 filaments).
[b] Estimated from fiber resistivity using correlation of Lavin et. al. [5].
[c] Measured by single filament tensile test (average of 25 filaments, 40 mm gauge length, corrected for system compliance).

A high carbon yield naphthalene-based mesophase pitch (AR mesophase, lot 2W24, produced by Mitsubishi Gas Chemical Co., Inc.) was chosen as the matrix precursor. The anisotropic content of this pitch was 100% and its softening point was 252°C. The naphthalene-based mesophase pitch also is highly graphitizable and, thus, it would appear to be an attractive matrix material for carbon/carbon. Table 2 lists some of the typical material properties of the AR mesophase pitch.

Table 2. Chemical and physical properties of naphthalene-based AR mesophase pitch produced by Mitsubishi Gas Chemical Company (6).

Softening Point	251°C
Anisotropic Content	100 %
H/C ratio (atom/atom)	0.61
Specific Gravity	1.26 ~ 1.30
Fluorine Content	1.7 ppm
Ash Content	4 ppm
Solubility by Soxhlet-extraction	
Heptane Insoluble	98 %
Toluene Insoluble	71 %
Pyridine Insoluble	49.5 %

3. EXPERIMENTAL PROCEDURE

3.1 *Material preparation*

Although the AR mesophase pitch was 100% anisotropic, it had a significant fraction of low molecular weight components (29% toluene soluble [6]) which volatilize at 350°C. Past work has shown that if these components volatilize during composite fabrication, the resulting composite porosity can be as high as 50% [7]. To remove the lower molecular weight components, the raw AR pitch was heat treated. This involved crushing the pitch into a powder using a BRAUN one-cup coffee grinder. Next, the ground pitch was poured into a large crucible and then placed in a Vacuum Atmospheres high temperature vacuum oven. The oven temperature was ramped at 20°C/min to 350°C. The pitch was soaked at temperature for two hours under nitrogen at a pressure of 0.1 torr.

The vacuum heat treatment reduced the mass of the naphthalene-based mesophase by 15%. Vacuum heat treatment also changed the viscous behavior of the naphthalene-based pitch (see Figure 1), raising its softening point to 330°C and increasing the temperature dependence of its viscosity. However, perhaps the most significant effect of heat treatment was that the carbon

yield at 800°C increased from 65% to 85%. To differentiate the heat treated naphthalene-based mesophase from the original material (AR), the heat treated variety will be referred to as AR-120.

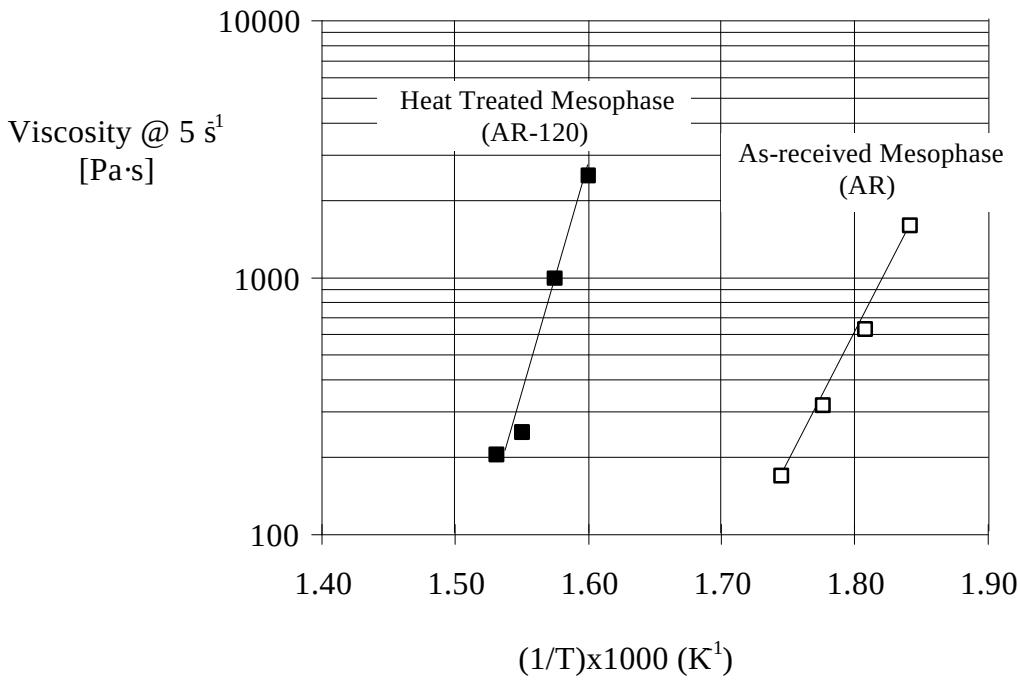

Figure 1. The effect of temperature on the melt viscosity of AR mesophase pitches at a shear rate of 5 s^{-1}.

3.2 *Towpreg formation*

Two types of carbon fiber towpreg were produced using the powder coating line illustrated in Figure 2. Amoco T300 PAN-based and P55 pitch-based carbon fibers were coated with heat treated AR mesophase pitch (AR-120), forming towpregs designated T300/AR-120 and P55/AR-120. Three areas in the process were critical for the production of a flexible towpreg: tow spreading, powder deposition, and powder fusion.

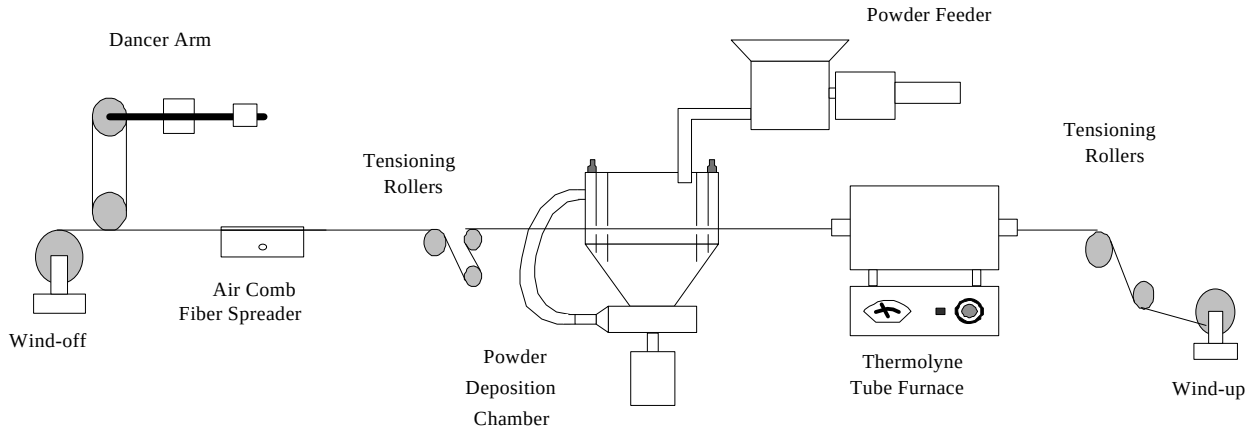

Overall schematic of powder coating process.

3.2.1 *Tow spreading.* To produce a flexible towpreg suitable for weaving, braiding, or knitting, the coating process must coat individual filaments in the tow, because coating the entire bundle encapsulates the tow, yielding a stiff prepreg. A pressurized air-comb was employed to separate the tow bundle during the coating process, as shown in Figure 3. With only 122 kPa air pressure, the air-comb was able to gently spread the tow to a width of about 8 cm, exposing the individual filaments of the tow for subsequent powder deposition. During this study, the tow speed through the coating process was held constant at 3 m/min.

3.2.2 *Powder Deposition.* Another critical area in the coating process was the powder coating technique itself. Unlike most other powder coating processes, which use static deposition and acoustic vibrational techniques, this process utilized a recirculating fluidized bed to deposit the pitch powder on the spread tow (Figure 4). During operation, dry pitch powder was fed into the chamber in a region of low air velocity and then fell toward a centrifugal fan. The fan fluidized

the powder and recirculated it to the chamber where it was deposited on the individual filaments of the spread fiber tow.

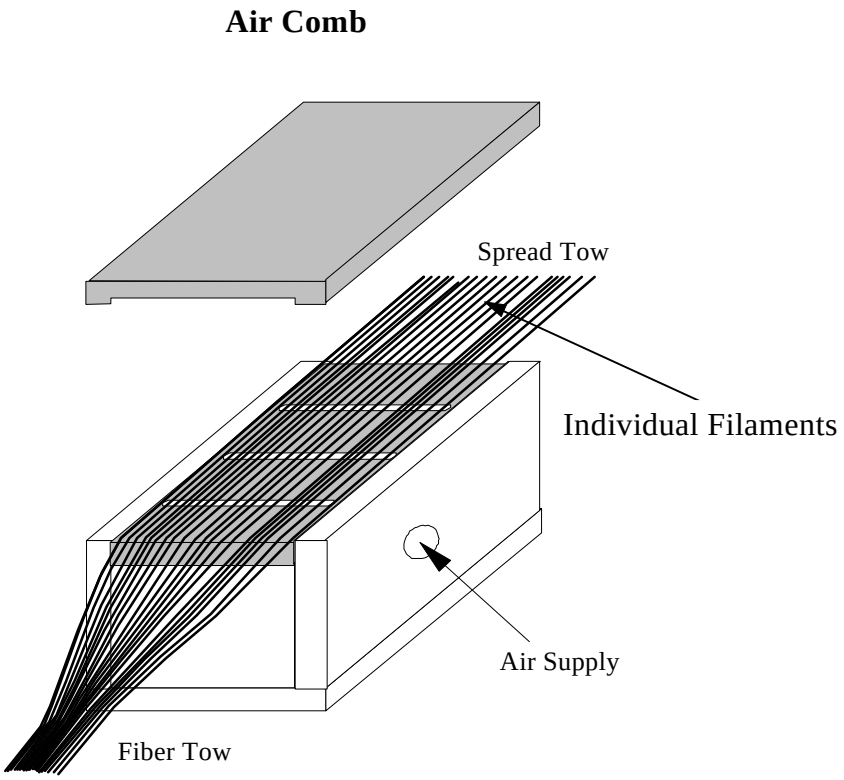

Figure 3. Schematic of air-comb fiber spreader.

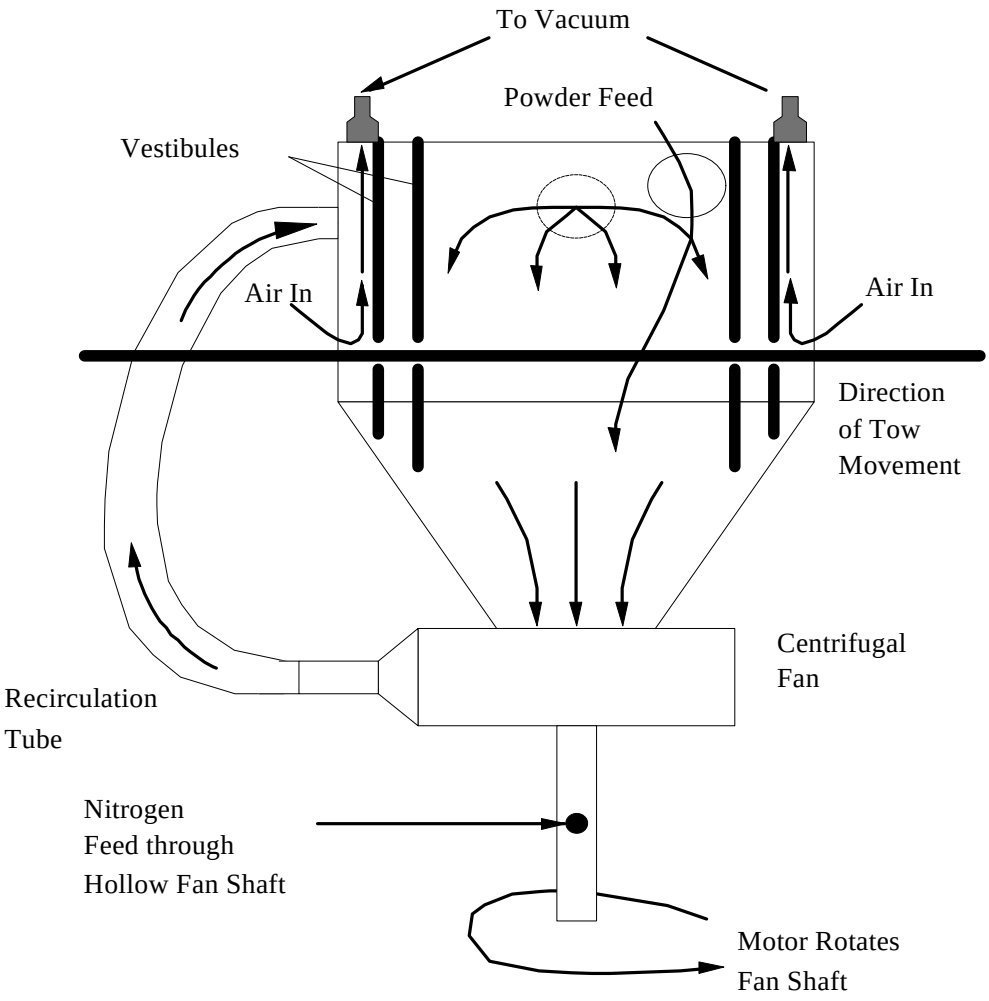

Figure 4. Detail of powder deposition chamber.

Earlier studies showed that optimum coating occurred when the powder size and fiber diameter were of the same order-of-magnitude [7]. Therefore, the treated pitch was crushed and passed through a 20μm sieve, yielding a pitch powder with a 10μm average particle size.

3.2.3 *Powder Fusion.* In order to adhere the powder to the individual filaments, the coated tow was passed through a tube furnace where it was heated to a temperature approximately 50°C above the softening point of the pitch. Earlier studies had shown that this temperature was sufficient to fuse the powder to the fibers [7]. When the oven temperature was excessively high, the powder completely melted and wet the fibers. The result was a stiff towpreg [2, 7] which could not be woven.

Unfortunately, the experimental ribbon-shaped fibers were supplied in lengths of nine inches, far too short for the powder coating process. Therefore, a manual procedure was developed to powder coat these short fibers. The technique involved separating the ribbon fibers and holding them over a dish. Next, the AR-120 pitch powder was dusted over the spread fibers. Shaking and hand manipulation were performed until a visually uniform coating was achieved. The coated ribbon fibers then were consolidated, following the same procedure employed for the T300 and P55-based towpregs.

3.3 *Composite fabrication*

All of the carbon/carbon composites were formed with a four step process. The towpreg was wrapped on a mandrel, placed in an open-ended mold and consolidated, forming a green composite. Then, the green composites were oxidized and carbonized to form the final carbon/carbon specimens used in this work.

3.3.1 *Composite lay-up and consolidation.* A wrapping mandrel was employed to facilitate lay-up of the coated T300 and P55-based towpregs. The towpreg was wrapped around the mandrel and then placed in an open-ended u-shaped mold tool to consolidate the towpreg into a 1.28 cm x 24 cm x 0.159 cm composite. Next, the mold was placed in a hot isostatic press and consolidated at a pressure of 6.8 MPa. Earlier work has shown that the towpreg can be fully consolidated, with a minimal amount of flash, if the pitch viscosity is approximately 200 Pa-s (at 5 s^{-1}) [7]. To achieve this viscosity and ensure adequate flow, the mold was heated to 380°C at 28°C/min. Then, the mold was cooled to room temperature after a 30 minute soak time (Figure 5).

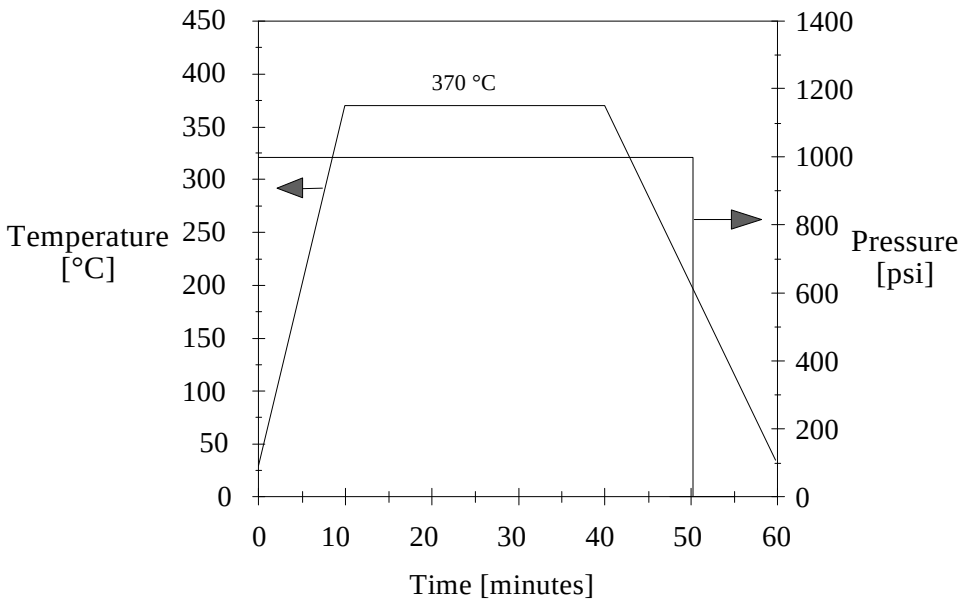

Figure 5. Cycle used to form T300, P55 and ribbon fiber towpreg into green carbon/carbon composites.

3.3.2 *Oxidation.* A thermogravimetric analysis was performed on the AR and AR-120 pitches, and the results are illustrated in Figure 6. As can be seen, the heat treated naphthalene-based pitch begins to react with oxygen at approximately 220°C. Thus, its oxidation temperature is similar to that of many petroleum pitches [8, 9]. Therefore, in this study the stabilization procedure consisted of placing the consolidated composites in a convection oven. The oven circulated air (heated to a temperature of 220°C) over the composite specimens for a period of 96 hours. During this process the mass of each composite sample increased to approximately 6% (depending on thickness and fiber fraction).

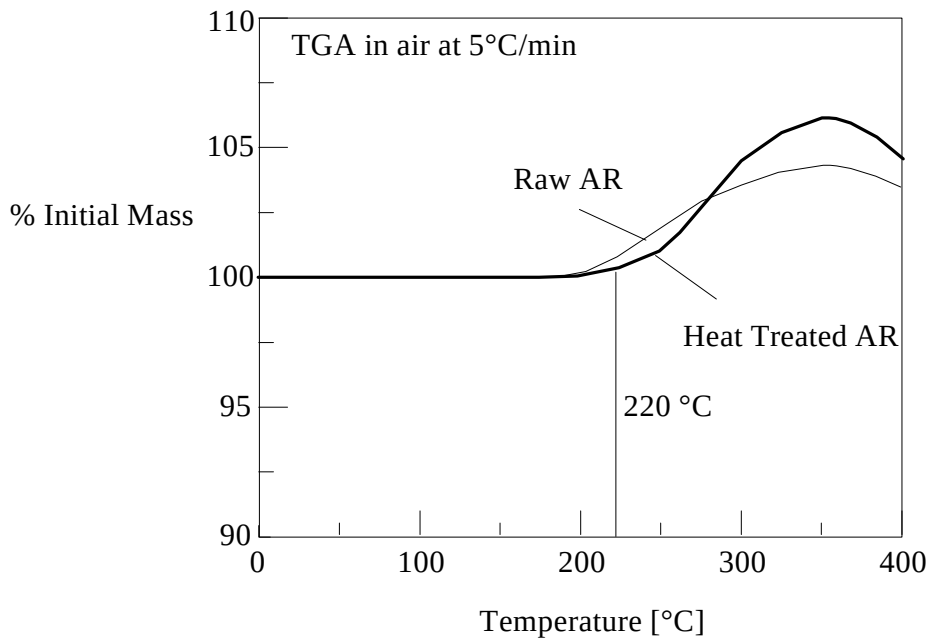

Figure 6. TGA analyses of as-received AR mesophase pitch and heat-treated AR-120 mesophase pitch showing mass gain with exposure to air.

3.3.3 *Carbonization.* The composite samples were carbonized in a Lindberg® ceramic box furnace, under a continuous purge of nitrogen. A heating rate of 0.5°C/min was used in order to minimize the formation of shrinkage cracks and slit pores caused by the thermal expansion mismatch between the fibers and the pitch.

3.3.4 *Graphitization.* A portion of the T300/AR-120, P55/AR-120, and ribbon/AR-120 composites were graphitized in a high-temperature Astro furnace at 2400°C with a heating rate of 20°C/min and under a continuous helium purge. After graphitization, the composites were cooled to room temperature at 20°C/min.

3.3.5 *Densification and re-carbonization.* Unfortunately, the coating uniformity of the ribbon-fiber towpreg was inferior to that of the T300/AR-120 and P55/AR-120 towpregs. This was most likely the result of the manual technique used to coat these experimental fibers. Because of their non-uniform coating, the carbonized ribbon fiber composites had very high porosities. Therefore, to increase their density, they were re-impregnated with raw AR mesophase. This involved covering the composites with mesophase pitch powder and heating them to 350°C under nitrogen at 300 psig. The composites were soaked in the liquid pitch under pressure for two hours, then oxidized and carbonized following the same procedure as before.

3.4 *Composite characterization*

3.4.1. *Flexural modulus and strength.* The flexural modulus of each group of specimens after carbonization and graphitization was determined following the ASTM D-790 four-point test procedure [10]. The tests performed in this research employed a four-point test fixture with a

span-to-depth ratio greater than 80:1 and deflections significantly less than 10% of the support span [11, 12].

3.4.2. *Thermal conductivity.* The thermal diffusivities of the samples were measured using a laser flash diffusivity test [13] at Oak Ridge National Laboratory in the Carbon Materials and Technology Group. The composites, arranged both parallel and transverse to the fibers, were machined into pellets with a diameter of 12 mm and thicknesses ranging from 6 to 10 mm. The density, ρ, was measured and the specific heat, C_p, was estimated at 684 J/g·°C. The thermal conductivity,κ, was calculated by the product of the diffusivity, the density and the specific heat.

4. RESULTS AND DISCUSSION

4.1. Towpreg Formation

4.1.1. *Tow spreading*. The air comb caused much less fiber damage than other vacuum and pressurized spreaders evaluated in previous research [7]. Also, twists in the feed tow did not interrupt the spreading. Thus, unlike other fiber spreaders, continuous monitoring by an operator was not required. The uniform spreading of the air comb was able to expose individual filaments for subsequent coating, resulting in a very flexible towpreg.

4.1.2. *Powder deposition.* The humidity within the coating chamber was found to be critical. To avoid problems associated with agglomeration, the powder in the chamber had to be free of moisture. Agglomerated powder resulted in an uneven distribution of polymer on the tow and, thus, produced a stiff and non-uniform towpreg. Optimum coating was obtained when the powder size and the fiber diameter were similar. If the powder particles were significantly larger than the diameter of the fibers, very little powder adhered to individual fibers and the resulting towpreg had a mottled appearance.

Figures 7 and 8 are SEM micrographs of stiff and flexible towpregs, respectively. In the stiff towpreg, many fibers were totally encapsulated by pitch. By comparison, in the flexible towpreg, the powder was fused to individual filaments.

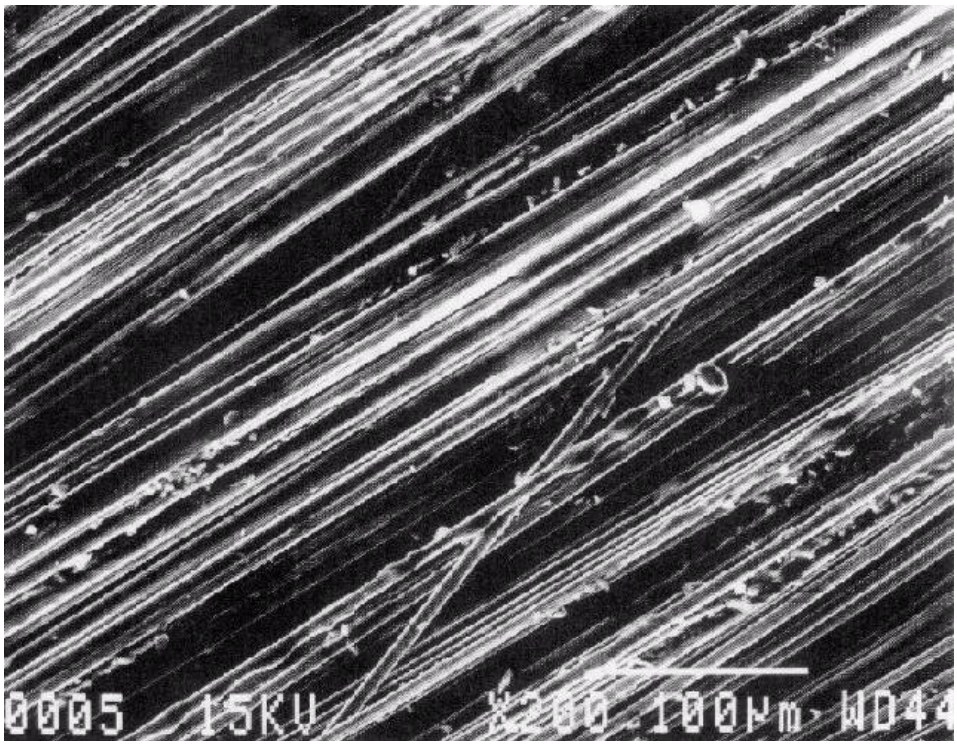

Figure 7. Scanning electron micrograph of a stiff towpreg.

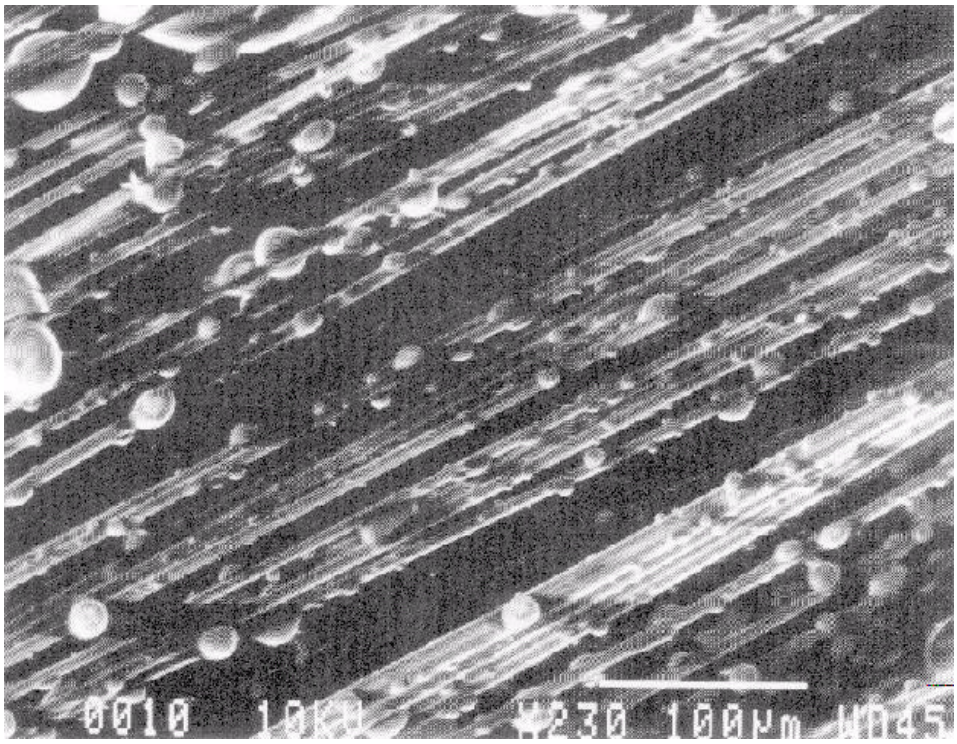

Figure 8. Scanning electron micrograph of a flexible towpreg.

4.1.3. *Powder fusion.* It was found that when the oven temperature was greater than 50°C above the pitch softening point, the pitch powder completely melted, encapsulating the entire fiber in a sheath of pitch. Often several fibers were encapsulated together, creating a minicomposite. The end result of this extensive wetting was a stiff, non-weavable towpreg. On the other hand, when the oven temperature was adjusted correctly, 50°C above the softening point of the pitch, the powder only adhered to the fiber at the point of contact. This avoided encapsulation of multiple filaments and yielded a flexible, weavable towpreg.

4.2. Composite Fabrication

4.2.1 *Composite consolidation.* More than 70% of the green composites formed with the T300/AR-120 towpreg had porosities less than 1%, and all had densities greater than 1.5 g/cc. This indicated that during the consolidation process, the pitch was sufficiently fluid to fill the gaps between the fiber bundles. This characteristic is extremely important, if towpreg is to be successfully used for multidimensional preforms.

4.2.2 *Carbonization and graphitization*. Carbonization of the oxidized T300/AR-120 composites at 1100 °C resulted in composite densities ranging from 1.4 to 1.64 g/cc with an average of 1.54 g/cc (see Figure 9). The fiber volume fraction ranged from 44% to 74% with average of 56%. However, graphitization at 2400°C resulted in an increase of the average density to 1.69 g/cc (ranging from 1.5 to 1.8 g/cc). The porosities ranged from 4% to 25% at both heat treatment temperatures (see Figure 10), with the low porosities corresponding to composites with high fiber volume fractions. This was a significant improvement over the 20% to 60% porosities for composites previously formed from T300 fibers and unstabilized, raw AR mesophase pitch

produced in an earlier study [7]. In fact, most of the commercial composites also have porosities ranging from 4 to 25%. However, nearly all of these commercial composites have undergone several densification cycles [14, 15, 16]. Thus, by comparison, the specimens made in the present research are excellent, given the short fabrication time.

The carbonized P55/AR-120 composites had densities ranging from 1.4 to 1.66 g/cc with an average of 1.57 g/cc. The fiber volume fraction ranged from 46% to 52% with an average of 55%, very similar to the T300/AR-120 composites. However, unlike that in the T300/AR-120 composites, the densities of this variety of composite did not change significantly when graphitized at 2400°C (see Figure 11). At both heat treatment temperatures, the porosities of the P55/AR-120 composites ranged from 12% to 27% (see Figure 12). While the range of densities and porosities for the P55/AR-120 and T300/AR-120 composites differed considerably, the scales used for Figures 9 and 10 were also used in Figures 11 and 12 to facilitate direct comparison of the data.

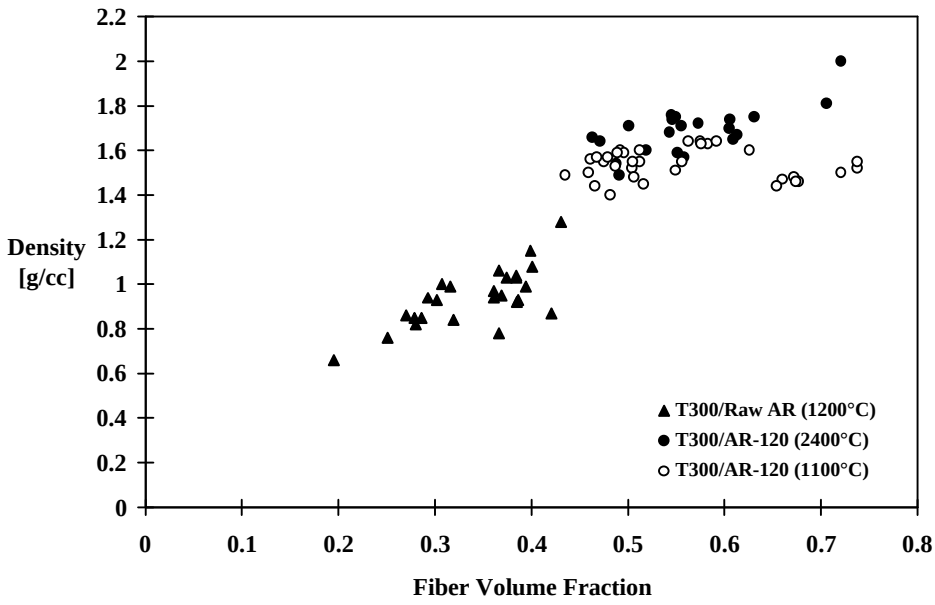

Figure 9. Density versus fiber fraction for carbonized and graphitized composites made from T300 carbon fibers coated with as-received (AR) mesophase and with heat-treated (AR-120) mesophase.

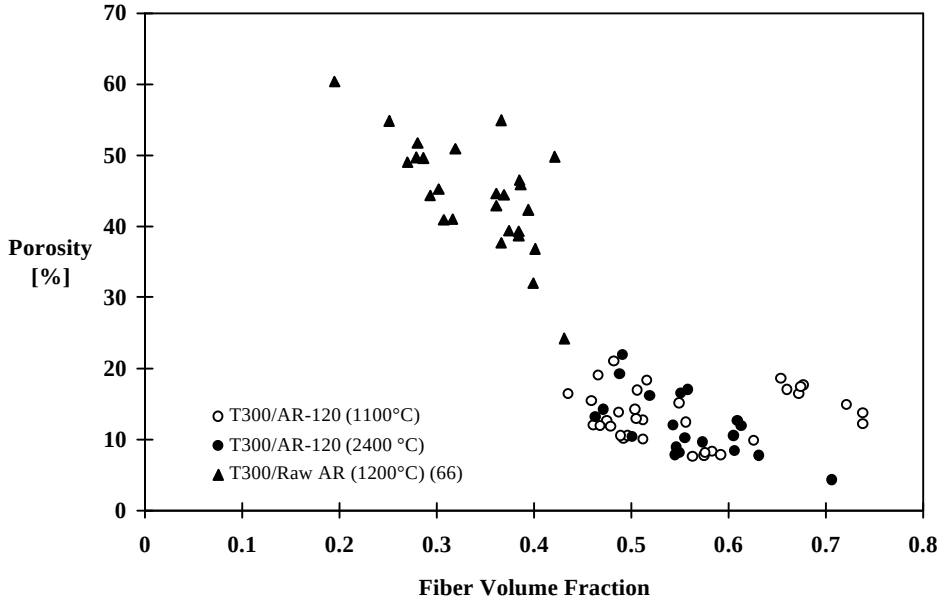

Figure 10. Porosity versus fiber fraction for carbonized and graphitized composites made from T300 carbon fibers coated with as-received (AR) mesophase and with heat-treated (AR-120) mesophase.

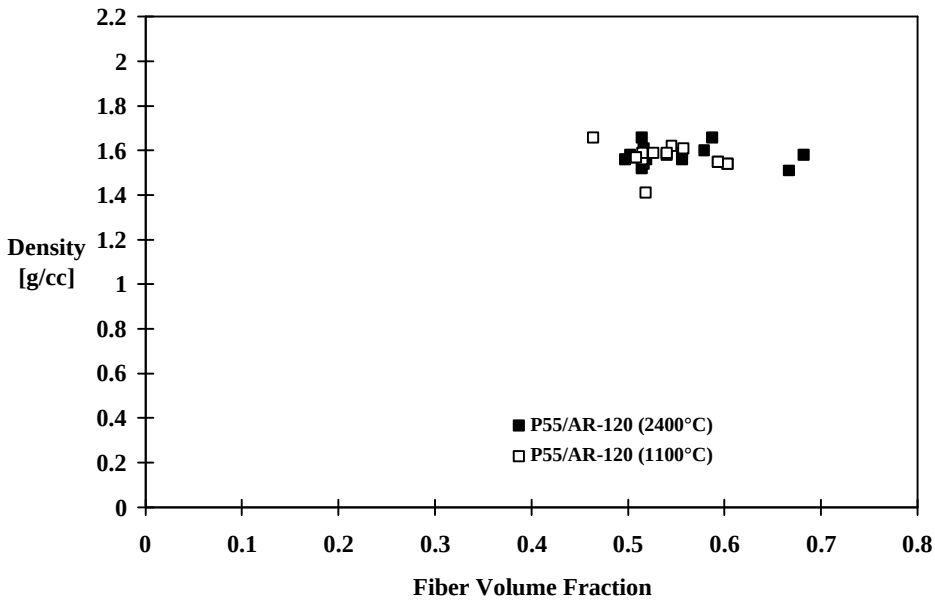

Figure 11. Density versus fiber fraction for carbonized and graphitized composites made from P55 carbon fibers coated with heat-treated (AR-120) mesophase.

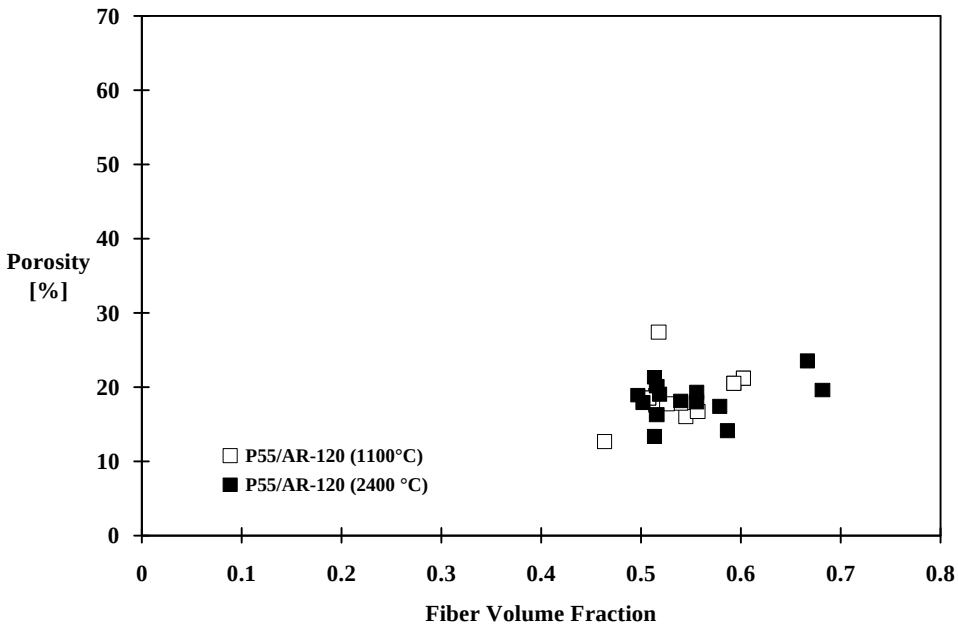

Figure 12. Porosity versus fiber fraction for carbonized and graphitized composites made from P55 carbon fibers coated with heat-treated (AR-120) mesophase.

4.3 *Microscopic evaluation*

4.3.1. *T300/AR-120 composites* Figures 13 (a) and (b) are cross-polarized light micrographs of T300/AR-120 composites heat treated at 1100°C and 2400°C, respectively. The micrographs show that during heat treatment, the mesophase pitch matrix preferentially oriented parallel to the fiber axis in a sheath-like structure around the fibers. In addition, a typical flow-like domain texture [14] can be seen in matrix-rich regions of the composites heat treated at 1100°C. Figure 14 illustrates the sheath-like structure that tends to form in a pitch matrix precursor during carbonization. Some authors attribute this to flow orientation [7, 8, 17, 18].

During graphitization the matrix appears to transform from flow-like domains to mosaic folded domains. This conversion from flow texture to folded texture, caused by fold sharpening and layer-plane misalignment during graphitization [7], can be detected by cross-polarized light optical microscopy, provided the domain size is larger than 0.5 μm [14]. While folding and layer-plane misalignment probably was present in the flow domains of the 1100°C samples, the domain size most likely was smaller than the resolution of cross-polarized light optical microscopy. Thus, the regions appeared as flow texture. This increased folding upon graphitization will most likely increase the strength of the matrix, but may inhibit the flow of heat in these regions.

As can be seen from Figures 13 (a) and (b), the cracks caused by shrinkage stresses during heat treatment developed primarily in the matrix and not at the fiber/matrix interface, with the cracks following parallel to the basal planes of the matrix. There was no significant fiber/matrix debonding in either the 1100°C or the 2400°C heat treated samples. This resulted in a significant bulk volume shrinkage of the composites during graphitization and, thus, an increase in composite

density. One might expect that this will translate into increased mechanical and thermal properties as well.

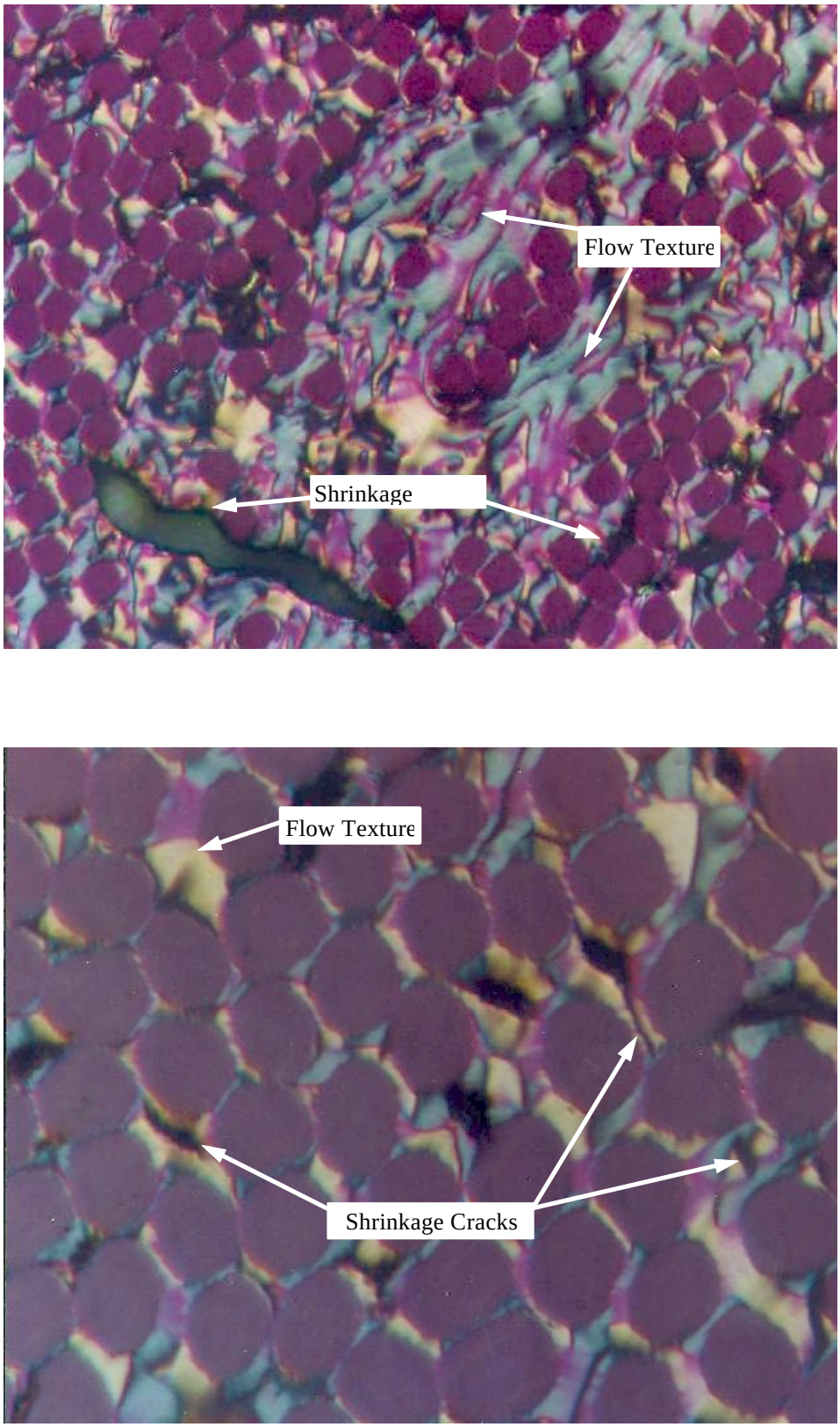

Figure 13a. Cross-polarized images of cross sections of a T300/AR-120 composite heat treated to 1100°C.

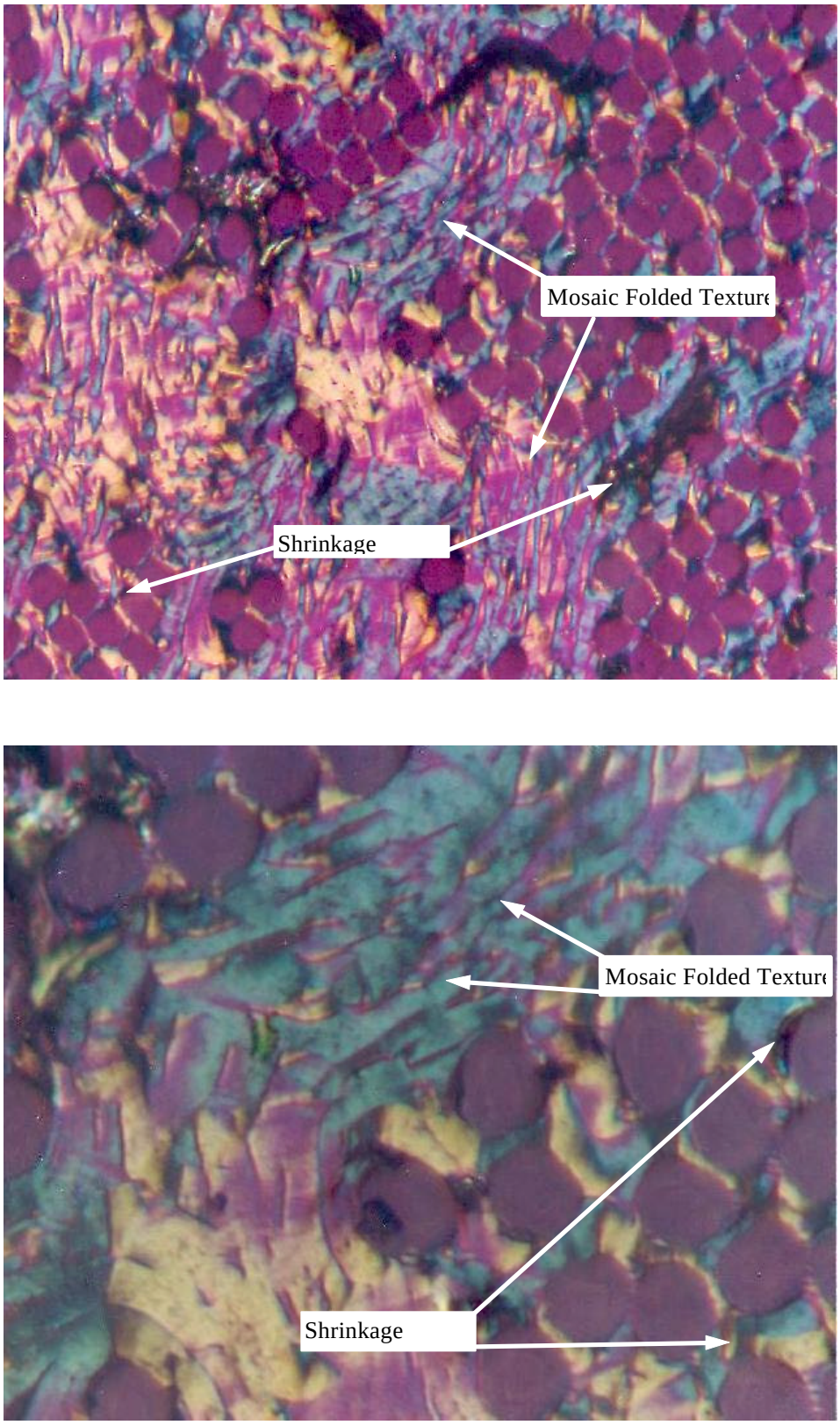

Figure 13b. Cross-polarized images of cross sections of a T300/AR-120 composite heat treated to 2400°C.

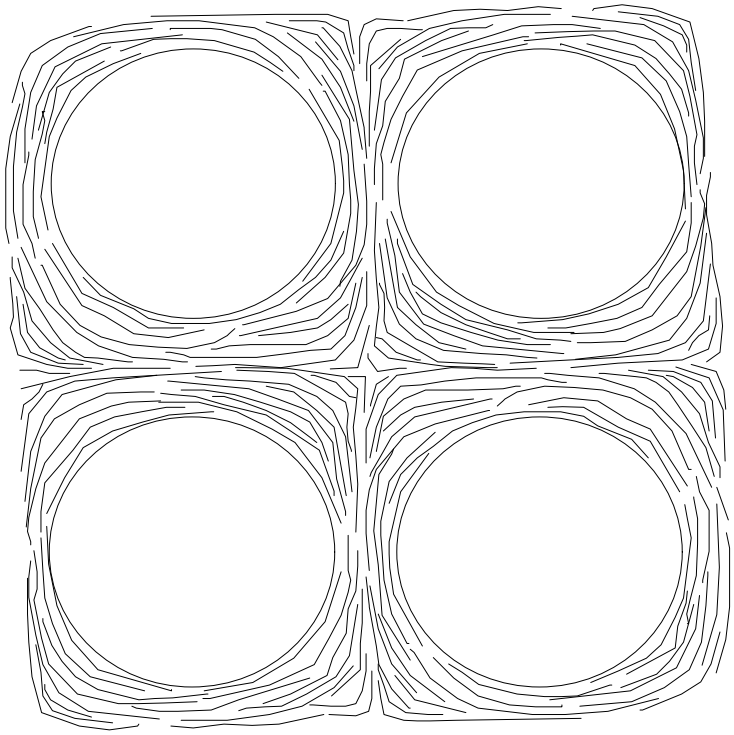

Figure 14. Illustration of the sheath-like orientation observed in pitch matrices which are reinforced with round PAN-based fibers.

4.3.2. *P55/AR-120 composites.* The mesophase pitch matrix oriented in a sheath-like structure around the P55 fibers as well. Thus, the matrix structure was quite similar to that observed in the T300/AR-120 composites. In addition, the P55/AR-120 composites exhibited the same conversion from a flow texture at 1100°C (Figures 15 (a)) to a mosaic texture at 2400°C (Figure 15 (b)).

However, unlike the T300/AR-120 system, the P55 fibers and the AR-120 matrix seemed to develop a very poor fiber/matrix interface. This extensive fiber/matrix debonding is typical for

pitch fiber composites. Their smooth surface texture and small number of surface functional groups [19] make it difficult for pitch fibers to form a strong fiber/matrix bond. In addition, the large differences between the thermal expansion coefficient of the fibers and of the matrix can create large differential shrinkage stresses. During carbonization, the weak interface bond strength, combined with shrinkage stresses, causes the matrix to debond from the fibers. Thus, the majority of shrinkage cracks developed at the fiber matrix interface, instead of in the matrix phase.

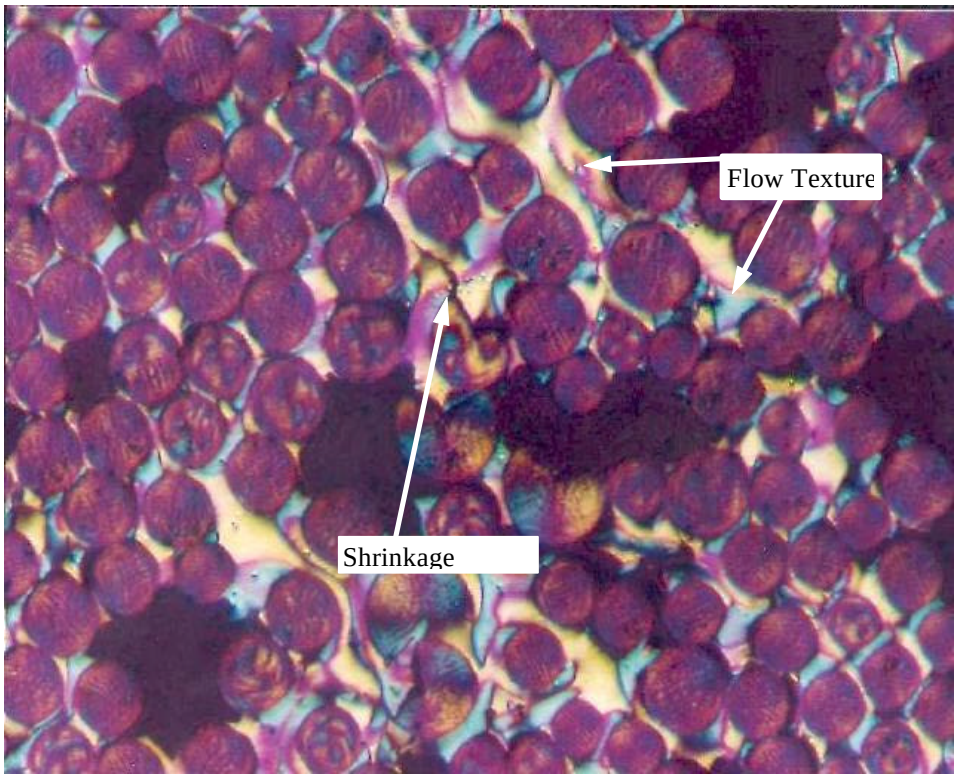

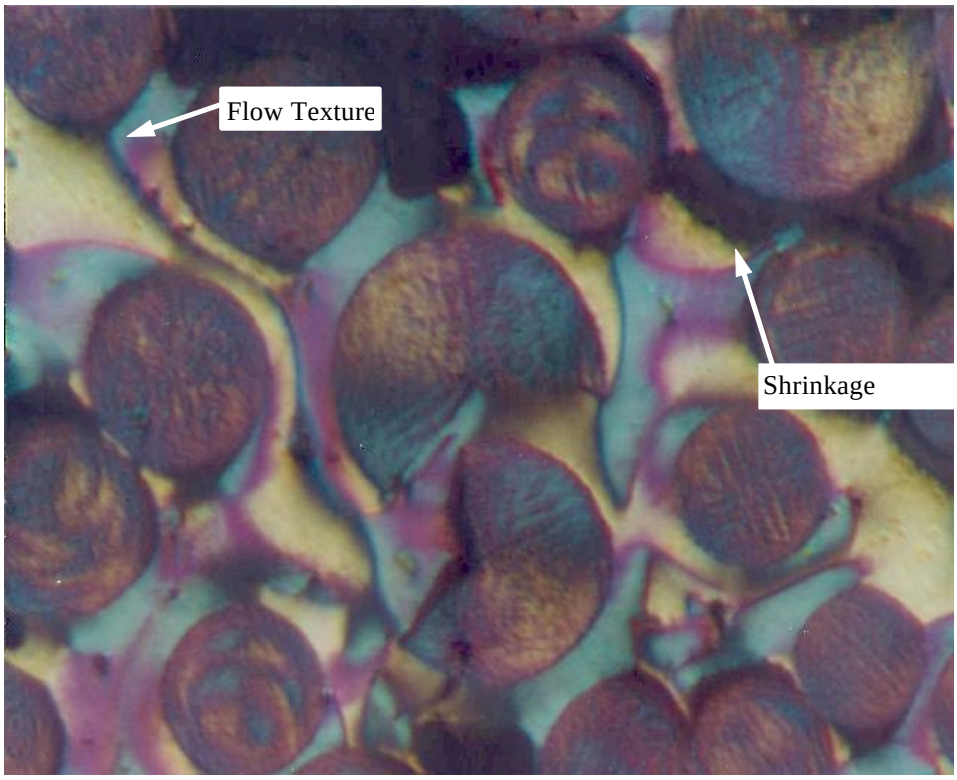

Figure 15a. Cross-polarized images of cross sections of a P55/AR-120 composite heat treated to 1100°C.

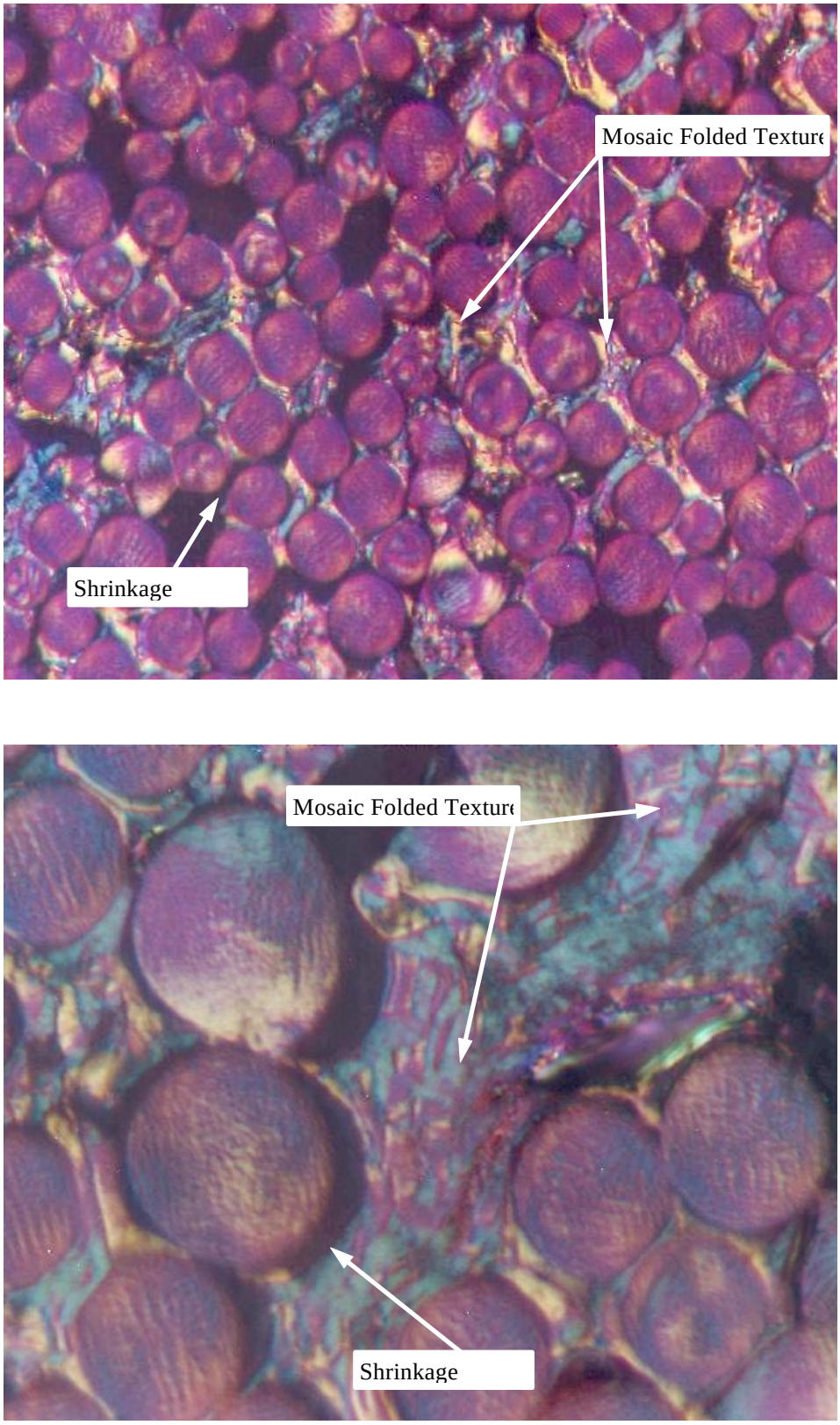

Figure 15b. Cross-polarized images of cross sections of a P55/AR-120 composite heat treated to 2400°C.

4.3.3. *Ribbon/AR-120 composites.* During processing, the ribbon fibers packed with the long direction of the fiber cross section oriented perpendicular to the pressing direction, except in the regions surrounding bubbles formed during pyrolysis (see Figures 16 (a) and (b)). This should allow ribbon fiber-based composites to achieve high fiber volume fractions during consolidation, perhaps even higher than those possible for round fibers.

As expected, the matrix oriented parallel to the surface of the fibers. However, very few mosaic textures were observed in the graphitized Type I ribbon-fiber composites, indicating that the matrix structure is more linear than that observed in the P55/AR-120 specimens. In addition, less curvature of the matrix around the ends of the fibers was observed, compared to that of the matrix in the P55/AR-120 composites. The matrix oriented almost entirely in the long direction of the fibers (perpendicular to the pressing direction). Even the matrix located in the spacing between the packed fibers, illustrated at (A) in Figure 17, was oriented parallel to the long direction of the fibers. This resulted in large flow-like domains of oriented matrix spanning several hundred microns, much more extensive than that observed in the carbon/carbon composites reinforced with round fibers. These large flow-like domains of matrix parallel to the long direction of the fibers should significantly increase the thermal properties of the composites. Apparently, this unusual matrix structure is a direct result of the high aspect ratio of the ribbon fibers.

Like the P55/AR-120 composites, the carbon/carbon composites reinforced with ribbon fibers had very little cracking within the matrix phase. This is because the ribbon fibers were not surface treated and had no sizing. Thus, fiber/matrix debonding was extensive. Since cracks could form easily at the fiber/matrix interface, few shrinkage cracks formed in the matrix phase. Ideally,

pitch-based fibers would be surface treated and sized. While this improves the interfacial bond, it inevitably causes shrinkage cracks to form primarily in the matrix phase.

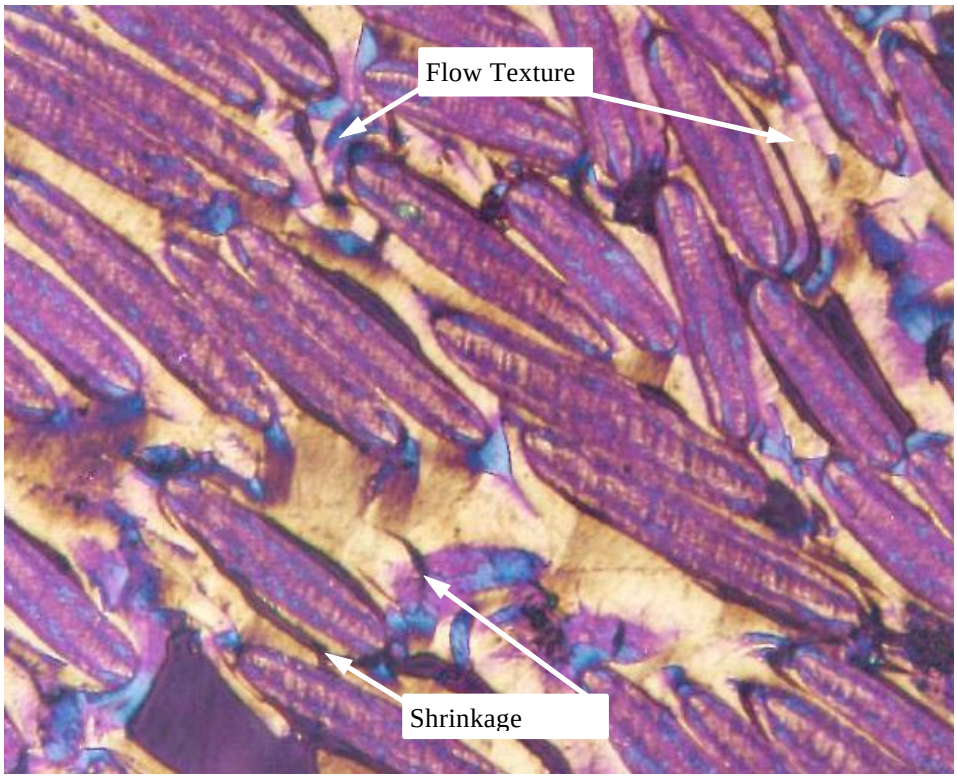

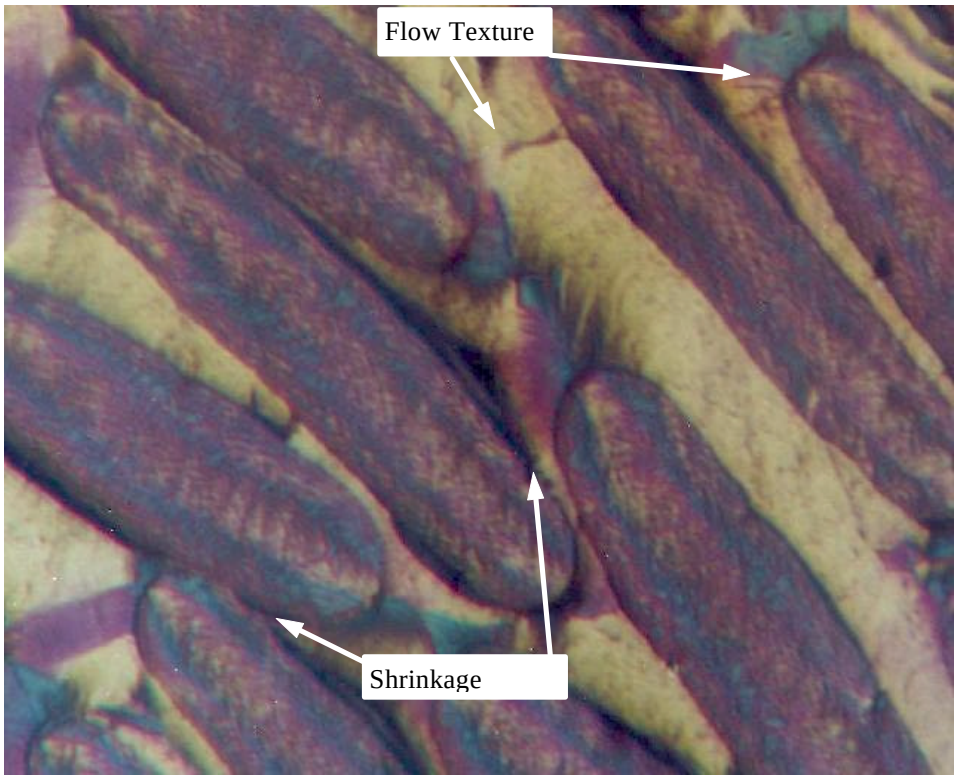

Figure 16a. Cross-polarized images of cross sections of a ribbon/AR-120 composite heat treated to 1100°C.

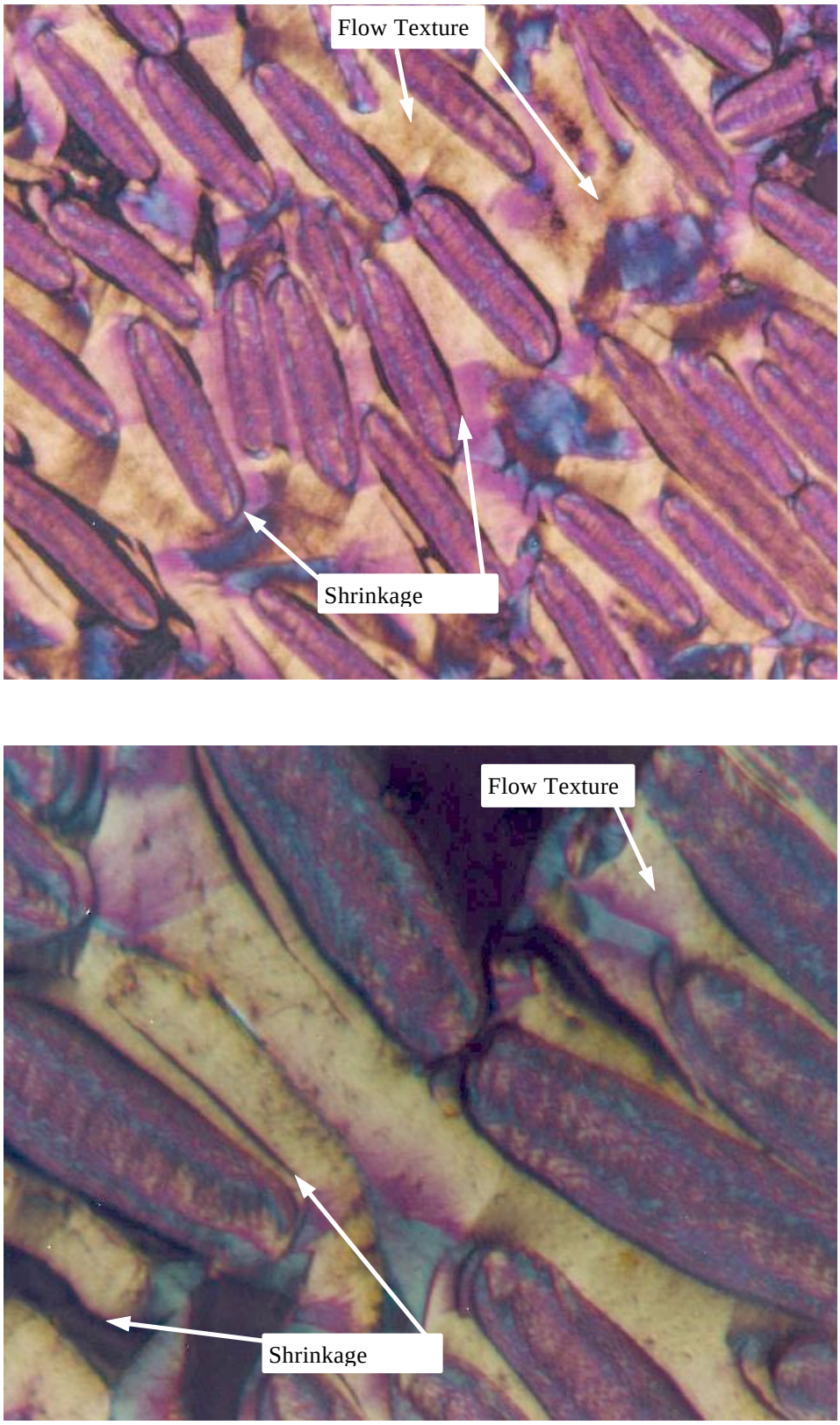

Figure 16b. Cross-polarized images of cross sections of a ribbon/AR-120 composite heat treated 2400°C.

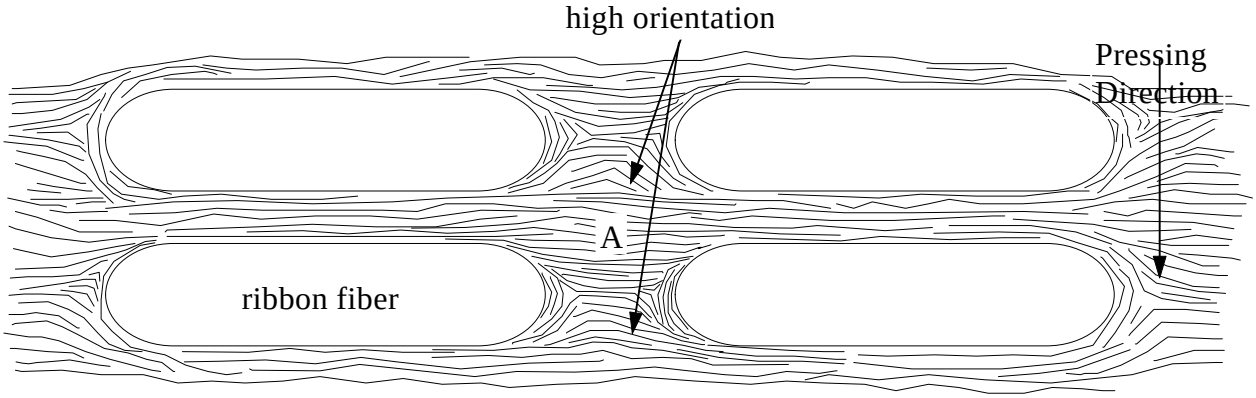

Figure 17. Illustration of the unique fiber and matrix orientation observed in composites reinforced with ribbon fibers.

4.4 *Mechanical Properties*

Table 3 contains the measured flexural moduli and flexural strengths of the T300/AR-120 and P55/AR-120 composites. At both heat treatment temperatures, the modulus of the composites was primarily a function of the fiber modulus. On the other hand, the strength of the composites was well below the expected translated strength. The translated strength is the ratio of the overall composite strength to the contribution of fiber strength predicted by the rule-of-mixtures (fiber fraction multiplied by the fiber strength). However, the rule-of-mixtures model that is commonly applied to composite materials assumes that the composite will fail at the failure strain of the fibers. The implicit assumption is that the failure strain of the fiber is much less than the failure strain of the matrix. While this assumption is valid for ductile polymer matrix composites, it is invalid for brittle matrix composites [20], e.g., carbon/carbon. In a carbon/carbon composite the brittle nature of the matrix, combined with residual stresses and pre-existing cracks formed during carbonization and graphitization, can cause premature failure of the composite. Moreover, the shear strength of graphite is typically an order-of-magnitude less than the tensile strength, and thus, shear stresses play a dominant role during composite failure.

Table 3. Mechanical properties of carbon/carbon composites formed from mesophase pitch-based towpreg and two different carbon fibers.

Composite Type	Final Heat Treatment Temperature (°C)	Fiber Tensile Modulus[a] (GPa)	Fiber Tensile Strength[a] (MPa)	Composite Flexural Modulus[b] (GPa)	Composite Flexural Strength[c] (MPa)	Failure Mode
T300/AR-120	1100	221	3.0	129 ± 30	691 ± 48	Non-catastrophic Tensile
	2400	302	1.8	196 ± 34	841[d]	Mixed Mode Shear/Tensile
P55/AR-120	1100	403	1.8	147 ± 50	162 ± 62	Buckling & Compression
	2400	500	2.1	216 ± 61	198 ± 8	Buckling & Compression

[a] Single Filament Testing (average of 25 filaments, 40 mm gauge length, corrected for machine compliance).
[b] Average of 8 samples.
[c] Average of 4 samples.
[e] Not enough failed in tensile failure to report standard deviation data.

Several researchers have studied the effects of the fiber/matrix interface on the mechanical properties of carbon/carbon composites [11, 21, 22, 23, 24]. Christ and Hüttinger, [21] performed an in-depth study of carbon/carbon composites made with an oxygen stabilized A-240 pitch matrix, reinforced with PAN-based carbon fibers. They also evaluated the effect of various surface treatments on the mechanical properties of carbon/carbon composites. They postulated that the fiber/matrix interface can be developed through either chemical bonding, physical bonding, or a combination of both. In the case of chemical bonding, the surface functional groups, primarily acidic carboxyl groups, form radicals during pyrolysis [21] and bond with the pitch. However, these groups are only indirectly responsible for the formation of a good fiber/matrix interface. During carbonization, the partially crosslinked matrix shrinks onto the

carbon fiber surface in a sheath-like manner. As the matrix shrinks, its grip on the fiber increases, further enhancing the fiber/matrix interface of the composites made with surface treated PAN-based fibers.

While the fiber/matrix interface appeared to be well developed in the T300 composites produced in this research, the fiber/matrix bond was, most likely, significantly weaker than that of typical polymeric composites [20]. The degree of fiber/matrix bonding, to a large extent, determines the ultimate strength of a carbon/carbon composite. A very poor fiber/matrix interface prevents load transfer from the matrix to the fibers and, thus, reduces the failure strength of the composite. Weak (or intermediate) bonding, by comparison, usually leads to fiber pull-out, an inherent toughening mechanism. However, an intermediate fiber/matrix bond can actually prevent further propagation of cracks. This occurs because the fiber/matrix interface will debond and the crack will propagate down the length of the fiber [18], absorbing fracture energy. This is repeated until all of the fiber/matrix interface is destroyed or until no more load can be supported [18]. On the other hand, a very strong fiber/matrix interface does not allow the interface to absorb the fracture energy and the cracks propagate through the fiber, causing the composite to fail in a more catastrophic-like tensile fracture [18, 19, 21]. Therefore, a intermediate fiber/matrix interface is desired - high enough to transfer load to the fibers, but low enough to prevent a crack from propagating through the fibers.

This influence of interfacial bonding on composite strength explains many of the trends observed in the current research. The carbonized T300/AR-120 composites had a well-developed fiber/matrix interface and, thus, exhibited excellent strengths (691 MPa). In fact, their average strength increased to 841 MPa upon graphitization. The translation of fiber strength to composite

strength also increased upon graphitization (41% to 85%), primarily because of increased bonding of the fiber/matrix interface (due to matrix shrinkage around the fibers) and reduced notch sensitivity (due to the increased folding and increased strength of the graphite crystals). However, along with the composite strength, the mode of failure also changed upon graphitization. The failure changed from a typical "pull-out" tensile failure for the carbonized samples to a combination of tensile and shear failure (mixed mode) for the graphitized samples. This most likely was a result of the increased fiber/matrix bonding caused by shrinkage of the matrix around the fibers during graphitization. This increased bonding increased load transfer to the fibers and, thus, increased the overall tensile strength of the composite. However, this same increased fiber/matrix bonding also made shear failure a more dominant mechanism and, thus, resulted in a mixed mode failure and a less tough composite.

By comparison, the fiber/matrix interface of the P55/AR-120 composites was much less developed. As previously mentioned, this trend is typically observed when carbon/carbon is reinforced with pitch fibers, because the fibers have a very smooth surface texture and relatively few surface functional groups. The P55/AR-120 composites failed under a combination of compression and buckling at both treatment temperatures. The poor fiber/matrix interface resulted in poor load transfer, and thus, the tensile strength of the composite (162 MPa) was only 16% of that predicted by the rule-of-mixtures.

Like the T300/AR-120 composites, the strength of the P55/AR-120 composites increased upon graphitization, achieving values of 192 MPa (17% translated strength). As previously mentioned, graphitization of the T300/AR-120 composites increased the interfacial bond strength and, thus, improved composite strength. However, the poor interfacial bonding makes this type

of improvement unlikely in the P55/AR-120 specimens. In fact, the increase was probably due to the increase in the fiber strength alone.

4.6. *Thermal properties.*

The thermal properties of the composites are listed in Table 4. Unfortunately, the properties of two composite types (1100°C T300/AR-120 transverse and 2400°C P55/AR-120 transverse) could not be measured because of the high heat flow transverse to the heat pulse.

After heat treatment at 1100°C, the thermal conductivity of the T300/AR-120 and P55/AR-120 composites (measured parallel to the fibers) was 4.86 and 70.8 W/m·K, respectively. Recall that, at both heat treatment temperatures, the porosities in the T300/AR-120 composites ranged from 4% to 25%, while the porosities in the P55/AR-120 composites ranged from 12% to 27%. This indicates that in both types of composites heat treated to 1100°C most of the heat was transferred by the fibers, corroborating the observation that heat treatment at 1100°C did not fully develop the matrix structure. However, after heat treatment at 2400°C, the thermal conductivity of the composites (measured parallel to the fibers) increased significantly. This indicates that a largely graphitic structure was developed in the matrix at higher heat treatment temperatures.

Table 4. Thermal properties of carbon/carbon composites formed from mesophase pitch-based towpreg and three different carbon fibers.

Composite	Fiber Thermal Conductivity (W/m·K)	Final Heat Treatment Temperature (°C)	Parallel Thermal Conductivity (W/m·K)	Transverse Thermal Conductivity (W/m·K)
T300/AR-120	8.5[a]	1100	4.86 ± 0.21[c]	---
	76[b]	2400	80.5 ± 2.7[c]	6.86 ± 1.44[c]
P55/AR-120	113[b]	1100	70.8 ± 3.7[d]	2.40 ± 0.40[d]
	196[b]	2400	135.5 ± 4.3[d]	---
Type I ribbon/ AR-120	236[b]	2400	148.2[e]	213.5[e]

[a] Amoco Product Data Sheet (thermal conductivity is below the valid region for the Lavin Relation [5]).
[b] Estimated from single filament resistivity data using the Lavin Relation [5].
[c] Average of more than 20 samples.
[d] Average of 4 samples.
[e] Tested only one sample.

The thermal conductivity of the graphitized T300/AR-120 composites (measured parallel to the fibers) was 80.5 W/m·K. This was higher than that of the individual fibers, 76 W/m·K. Thus, at 2400°C the degree of graphitization (in other words, the development of graphitic structure) within the matrix was significant. Hence, the thermal conductivity of the P55/AR-120 composites (measured parallel to the fibers) also increased upon graphitization (135.5 W/m·K). More importantly, the thermal conductivity in the direction perpendicular to the fibers for the graphitized samples, 6.86 W/m·K, was even higher than the thermal conductivity in the direction parallel to the fibers for the carbonized samples, 4.86 W/m·K. This result, while surprising, can be easily explained since, in the transverse direction, the matrix is the only continuous phase and, thus, responsible for most of the heat transfer. This high transverse conductivity of the graphitized samples (even compared to the conductivity of the carbonized samples, measured

parallel to the fibers) indicates that the matrix was highly ordered and very conductive to heat transfer after treatment at 2400°C. These thermal conductivities are comparable to those of carbon/carbon specimens produced by the CVD method. However, since the composites utilized in this research took a considerably shorter time to fabricate, they represent a significant improvement over conventional fabrication techniques.

The influence of matrix orientation on composite conductivity was even more apparent in the composites reinforced with ribbon fibers. Because of the packing effect, the matrix aligned parallel to the long direction of the fibers with large regions of order that were rarely observed in composites reinforced with round fibers. This alignment produced an extremely planar graphitic matrix structure (almost all of the matrix appeared to be oriented parallel to the long direction of the ribbon fibers). Unfortunately, since only a few composites could be fabricated, x-ray analysis could not be performed to corroborate this observation. However, it is believed that this unusual structure should allow the matrix to collapse to a smaller interplanar spacing upon graphitization, possibly making the matrix of the ribbon fiber composites more conductive to heat transfer than that of the round fiber composites. In ribbon fiber composites, the conductivity of the matrix transverse to the fiber direction might even be greater than that parallel to the fiber axis. This is because during graphitization, shrinkage stresses and the thermal expansion mismatch often cause intramatrix cracks to develop perpendicular to the fiber axis, impeding the flow of heat parallel to the fibers. An exaggerated illustration of this is shown in Figure 18. Figure 19, a photomicrograph of a cross section of a ribbon fiber composite, also shows this effect. Heat flow is uninterrupted parallel to these cracks (perpendicular to the fiber axis) and, thus, the conductivity of the matrix in this direction can be higher than the conductivity of the matrix

parallel to the fiber axis. This effect can be alleviated by re-impregnating the sample and closing the fissures. Once the fissure are closed, the heat path parallel to the fiber axis will be uninterrupted and a higher thermal conductivity parallel to the fiber axis will result. Table 5 is a list of thermal properties of a ribbon fiber composite made with Type II ribbon fibers. The thermal conductivities were measured in the three axis directions (x, y, and z). As can be seen, the conductivity parallel to the fibers, z-direction, was higher than that in either of the transverse directions, x and y. Also, the conductivity in the direction perpendicular to the long direction of the fiber cross section, x-direction, was an order-of-magnitude lower than the thermal conductivity parallel to the long direction of the fiber cross section, y direction. Thus, it can be inferred that the matrix has long-range order and is oriented parallel to the long direction of the fiber cross sections.

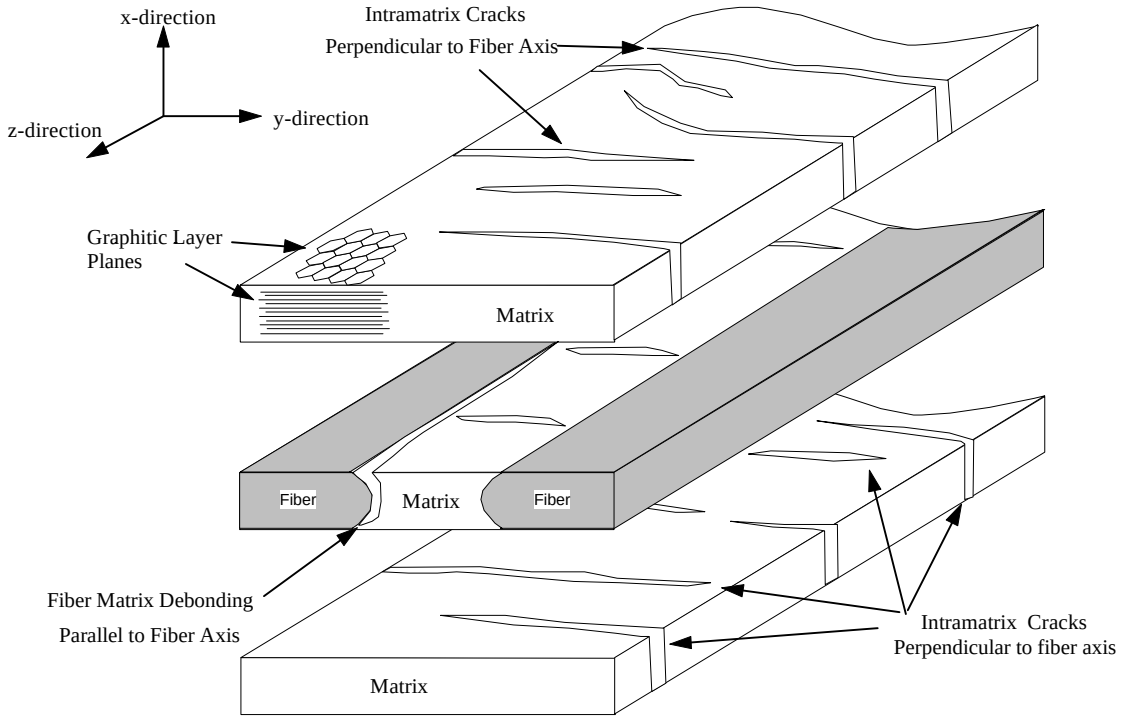

Figure 18. Schematic of intramatrix cracking and fiber-matrix debonding, both parallel and perpendicular to the fiber axis, in a ribbon/AR-120 composite.

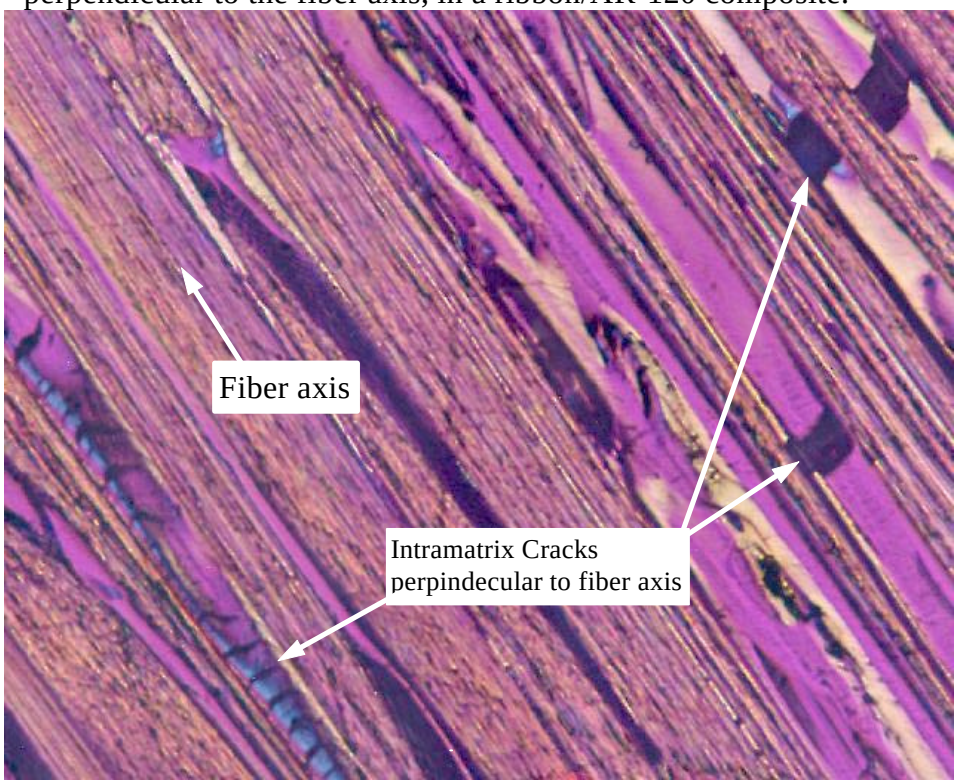

Figure 19. Photomicrograph of intramatrix cracking and fiber-matrix debonding, both parallel and perpendicular to the fiber axis, in a ribbon/AR-120 composite.

Table 5 Thermal properties of carbon/carbon composites formed from mesophase pitch-based towpreg and Type II ribbon fibers.

Composite	Fiber Axial Thermal Conductivity (W/m·K)	Final Heat Treatment Temperature (°C)	x-Direction Thermal Conductivity (W/m·K)	y-Direction Thermal Conductivity (W/m·K)	z-Direction Thermal Conductivity (W/m·K)
Type II Ribbon AR-120	429[b]	1100	0.82 ± 0.16	3.55 ± 0.87	90.13 ± 16.1[a]

[a] Average of 4 samples.
[b] Estimated from single filament electrical resistivity data [5].
NOTE: Conductivities are reported for the x, y, and the z directions defined in Figure 18.

This increase in graphitic structure was confirmed by x-ray studies in which the diffraction attributable to the matrix was deconvoluted from the overall diffraction pattern of the composite. Table 6 lists the crystalline parameters of the matrix and of the fibers for the graphitized T300/AR-120 composites. Since the diffraction pattern for the matrix of the carbonized composites was not resolvable, it can be assumed that the crystallographic structure in these samples was very disrupted. Thus, the x-ray results indicate that the matrix structure and alignment parallel to the fibers improved dramatically during graphitization.

Table 6. Crystallographic lattice properties of the matrix and fibers deconvoluted from the x-ray scans of T300/AR-120 composites.

Component	Final Heat Treatment Temperature (°C)	d_{002} spacing (nm)	Coherence Length, $L_{a,1010}$ (nm)	Stack Height, L_c (nm)
AR Matrix in situ	1100	not resolvable	not resolvable	not resolvable
	2400	0.338	36.8	170.6
T300 Fiber	1100	not resolvable	not resolvable	not resolvable
	2400	0.346	not resolvable	71.0

Several researchers have shown that the reinforcing fiber also can affect the matrix properties [22, 23]. Strong [22] has shown that the matrix will develop different degrees of graphitic structure depending on the type of fibers employed (e.g., PAN or pitch). Therefore, it is not unreasonable that the shape of the fibers will have an effect on the structure of the matrix. This appears to be the case because the transverse thermal conductivity of the ribbon/AR-120

composites is nearly two orders-of-magnitude greater than the transverse thermal conductivity of either the P55/AR-120 or the T300/AR-120 composites. In addition, composites made with ribbon fibers exhibit true three-dimensional anisotropy, with x, y, and z conductivities that vary by two orders-of-magnitude.

A conductive matrix is essential for composites used in thermal management applications. In order for the fibers to "wick" the heat away from a source, the matrix must transmit the heat to the fibers. Additionally, if the matrix is not conductive, large temperature gradients can develop across the composite. Large temperature gradients can create stress concentrations which, in turn, can damage the composite, further reducing the effectiveness of the composite for passive heat management.

4.6 *Composite fabrication using towpreg*

Pitch is currently being evaluated by many researchers [8, 9, 19, 24 - 30] as a matrix precursor for low cost carbon/carbon composites. However, its processability has been regarded as a major limitation in high volume applications. White and Gopalakrishnan [28] performed an extensive study using various petroleum pitches and determined that the processing window for melt impregnation is limited. This window is defined by the feasible processing temperature and upper and lower viscosity limits, as illustrated in Figure 20. During processing, the pitch must be heated to a temperature which is sufficient for flow and impregnation into the fine pores within the fiber bundles. However, if the pitch is heated above its degradation temperature, it will pyrolyze and solidify, preventing complete impregnation of the preform. An additional restriction is that the viscosity of the pitch must be high enough to prevent matrix cracks from closing during the

stabilization step. These cracks are necessary to allow complete penetration of oxygen through a thick multidimensional part. As can be seen, this window is quite small; thus, processing costs are more significant than material costs, making melt impregnation uneconomical for high volume applications.

The unique character of the pre-impregnated towpreg can expand this processing window significantly. Towpreg permits adequate consolidation of multidimensional parts, even at higher pitch viscosities than those required for conventional melt impregnation. This can shift the processing window outward, as shown in Figure 20. The viscosity-temperature curve for the AR-120 pitch matrix used in this research is plotted, and it can be seen that the curve falls well outside the processing window recommended by White and Gopalakrishnan [28]. This expanded window, combined with a short fabrication time, could allow carbon/carbon to enter high volume markets such as brake and clutch systems. The towpreg was woven into a fabric, Figure 21, to demonstrate the potential of this process for producing multidimensional carbon/carbon composites. Very little pitch matrix was lost during the process, indicating that pitch coated towpreg can be used to produce composites with multidimensional architectures (by weaving, braiding, knitting, etc.).

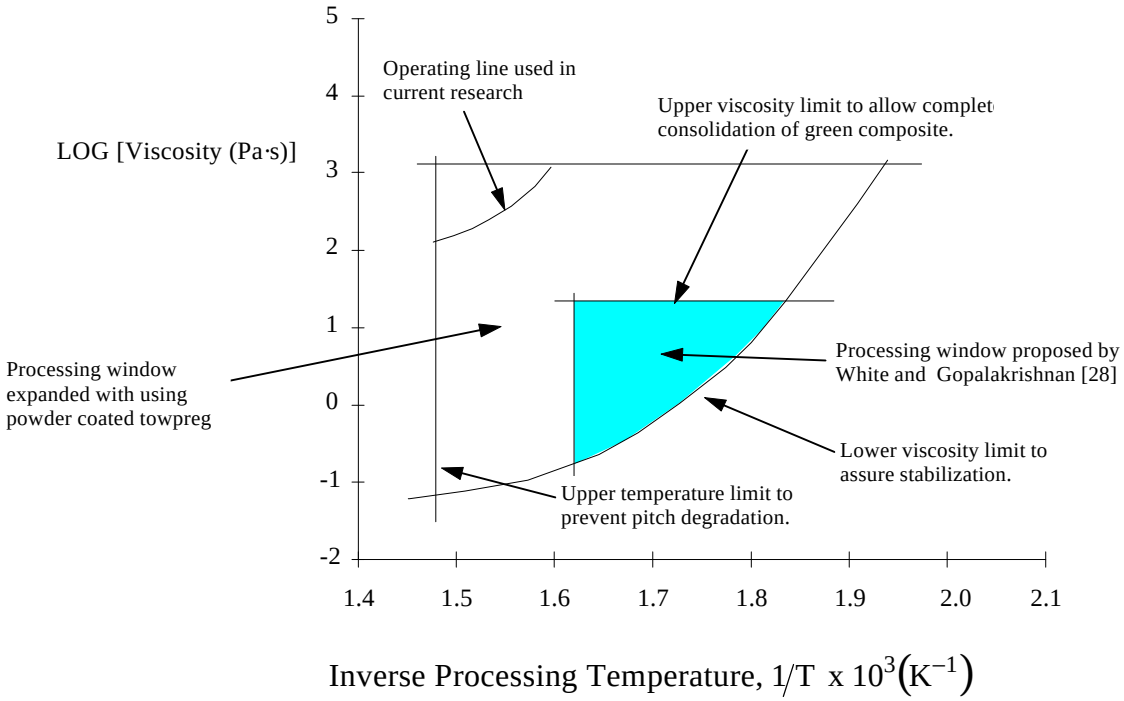

Figure 20. Processing window for fabricating carbon/carbon by melt infiltration [28] versus the expanded window available for forming carbon/carbon via towpreg.

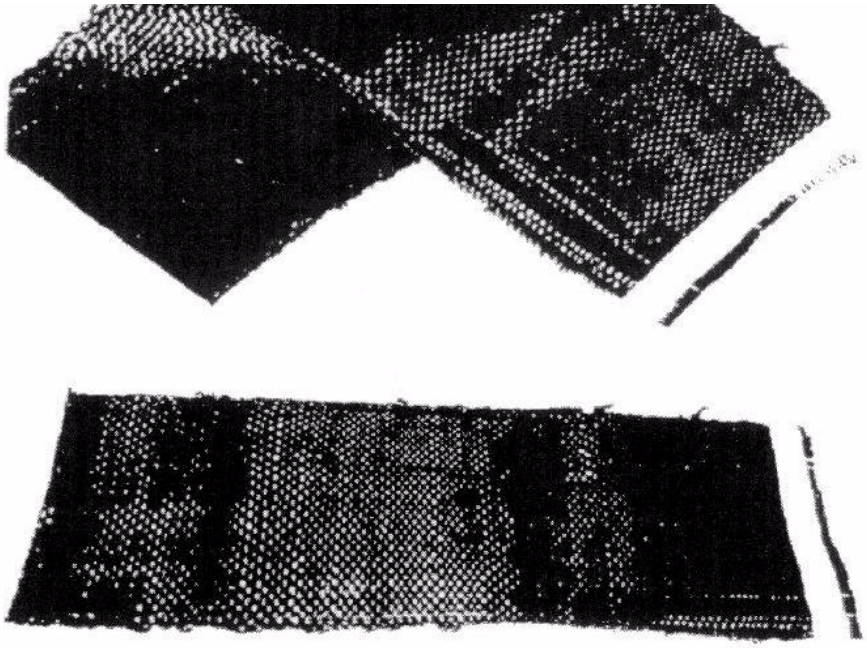

Figure 21. Fabric woven from mesophase pitch-coated towpreg.

5. CONCLUSIONS

Pre-heat treatment of the matrix precursor used in this research (AR 2W24 mesophase pitch) increased both the density (reduced porosity) and the carbon yield of the final carbon/carbon composites. Furthermore, it was shown that a strong fiber/matrix interface resulted in a high translation of fiber strength to composite strength, whereas a weak fiber/matrix interface resulted in a relatively low translation of fiber strength to composite strength.

The T300 fibers developed a strong fiber/matrix interface and the P55 fibers developed a weak fiber/matrix interface. Consequently, the composites fabricated with T300 fibers exhibited a flexural strength of 841 MPa and a flexural modulus of 196 Gpa. By comparison, the composites fabricated with P55 fibers exhibited a flexural strength of 198 MPa and a flexural modulus of 216 GPa. In addition, graphitization of the composites resulted in the preferred alignment of the basal planes, within the matrix, parallel to the fibers. Thus, the graphitized composites, with a pitch matrix, exhibited axial thermal conductivities comparable to those of composites produced by the CVD method.

During pressing of the composites, the ribbon fibers tended to orient with the long direction of the fiber cross section perpendicular to the direction of the applied force. This fiber orientation resulted in thermal conductivities transverse to the fiber axis which were two orders-of-magnitude greater than those measured for composites reinforced with round fibers. Additionally, the composites with the ribbon fibers exhibited three-dimensional anisotropy, while the composites with round fibers were essentially orthotropic.

The towpreg fabrication procedure can be used with pitches that are too viscous for conventional melt impregnation. Thus, the processing window can be expanded to include alternative pitches, which may form better composites in less time.

REFERENCES

1. L. E. Allen, *A Continuous Process for Powder Coating Carbon Fibers*, M.S. Thesis, Clemson University, Clemson, SC (1989).
2. B. W. Gantt, *Thermoplastic Coating of Carbon Fibers*, M.S. Thesis, Clemson University, Clemson, SC (1987).
3. Amoco Product Data Sheet (1988).
4. D. D. Edie, K. E. Robinson, O. Fleurot, S. P. Jones and C. C. Fain, *Carbon*, **32**, 1045 (1994).
5. J. G. Lavin, D. R. Boyington, J. Lahijani, B. Nysten, J.-P. Issi, *Carbon*, **31**, 1001 (1993).
6. Mitsubishi Product Data Sheet (1991).
7. J. W. Klett, *Towpreg Formation for Carbon/Carbon Composites*, M.S. Thesis, Clemson University, Clemson, SC (1991).
8. J. L. White and P. M. Sheaffer, *Carbon*, **27**, 697 (1989).
9. W. C. Stevens and R. J. Diefendorf, *Carbon '86, Proc. 4th Int. Conference On Carbon*, Baden-Baden, Germany (1986), pp. 37-38.
10. Standard Test Methods for "Flexural Properties of Unreinforced and Reinforced Plastics and Electrical Insulating Materials," Annual Book of ASTM Standards, Test D790 (1981).
11. C. W. Zweben, S. Smith, and M. W. Wardle, *Composite Materials: Testing and Design (Fifth Conference)*, New Orleans, March 20-22 (1978).
12. S. P. Appleyard, Ph. D. Thesis, University of Leeds, UK (1993).
13. W. J. Parker, R. J. Jenkins, C. P. Parker, C. P. Butler, and G. I. Abbott, *J. Appl. Phys.*, **32**, 1679 (1961).
14. N. Murdie, C. P. Ju, J. Don, and M. A. Wright, in *Carbon-Carbon Materials and Composites*, (edited by J.D. Buckley and D. D. Edie), pp. 105-167, Noyes Publications, New York (1989).
15. Fisher, Ronald, in *Essentials of Carbon-Carbon Composites*, (edited by C. R. Thomas), pp. 103-117, Royal Society of Chemistry, Cambridge (1993).
16. McAllister, L. E., in *Engineered Materials Handbook - Composites*, (edited by Theodore J. Reinhart), pp. 915-919, ASM International, Metals Park, Ohio (1987).
17. J. S. Evangelides, *Mat. Speak.*, **5**, 1 (1988).
18. E. Fitzer, W. Hüttner, and L. M. Manocha, *Carbon*, **18**, 291 (1980).
19. I. L. Loh, R. E. Cohen and R. F. Baddour, *J. Mat. Sci.*, **22**, 2937 (1987).
20. A. G. Evans, F. W. Zok and J. Davis, *Composites Science and Technology*, **42**, 3 (1991).
21. K. Christ and K. J. Hüttinger, *Carbon*, **31**, 731 (1991).
22. S. L. Strong, *Procedings of the 19th Biennial Conference on Carbon*, University Park, PA (1989), pp. 354-355.
23. N. Murdie, A. Langkamp, P. Stanek, J. Don, and M. A. Wright, *Carbon '92, Procedings of the 5th International Conference on Carbon*, Essen, Germany (1992), pp. 715-717.
24. E. Fitzer, K.-H. Geigl, and W. Hüttner, *Carbon*, **18**, 265 (1980).
25. E. Fitzer, *J. Chem. Phys.*, **81**, 717 (1987).
26. E. Fitzer, *Carbon*, **25**(2), 163 (1987).
27. M. S. Dresselhaus, G. Dresselhaus, K. Sugihara, I. L. Spain, and H. A. Goldberg, *Graphite Fibers and Filaments*, Springer-Verlag, Berlin, (1988).

28. J. L. White and M. K. Gopalakrishnan, *Procedings of the 20th Biennial Conference on Carbon*, Santa Barbara, CA (1991), pp. 184-185.
29. L. M. Manocha, O. P. Bahl, and Y. K. Singh, *Carbon*, **29**, 351 (1991).
30. I. Mochida, Y. Korai, A. Azuma, M. Kakuta, E. Kitajima, *J. Mat. Sci.*, **26**, 4836 (1991).